

Cold nuclear matter effects in J/ψ production

- Impact of the nuclear modifications of the parton densities
- Energy and rapidity dependence of $\sigma_{\text{abs}}(J/\psi)$
- Initial state parton energy loss
- Recent progress using EPS09

Hermine K. Wöhri
(LIP, Lisbon)

Nuclear effects in quarkonium production in p-A collisions

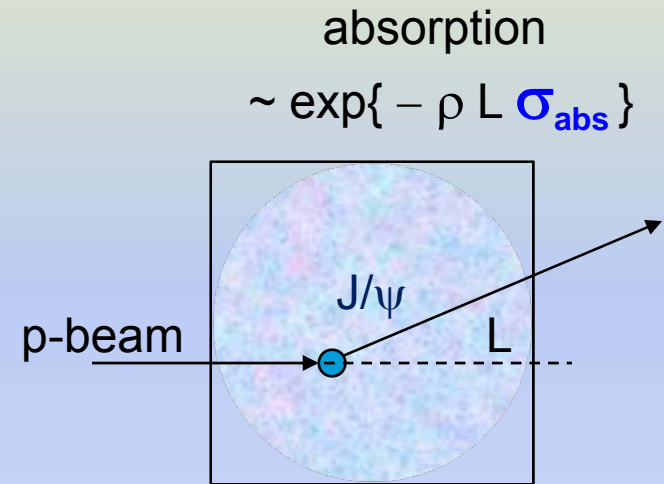
Several “cold nuclear matter effects” can modify the production of quarkonia in p-nucleus collisions with respect to pp collisions; in particular, we expect:

initial-state effects:

- nuclear modifications to the PDFs
- initial-state energy loss of incident partons

final-state effects:

- break-up of formed or pre-resonant charmonia (different for each charmonium state)

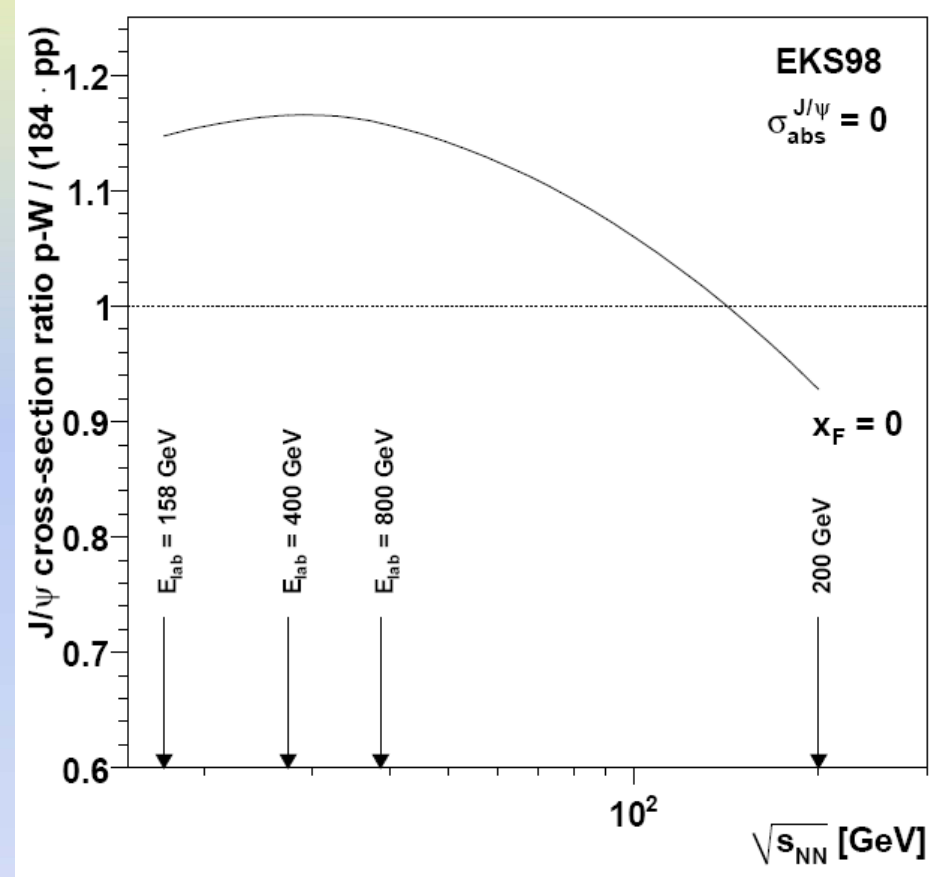
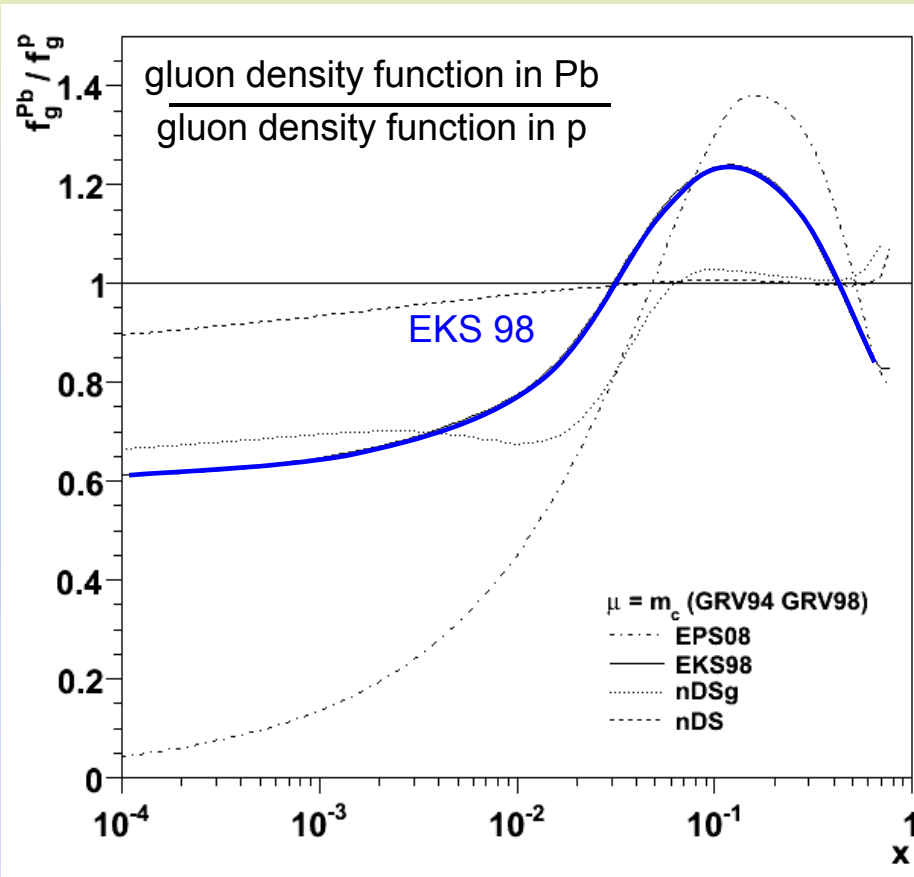


To understand these effects we need to study several data sets, collected in different kinematical domains, at different energies, with several nuclear targets, etc

And we need to consider the ψ' and χ_c measurements, together with the J/ψ results; around 1/3 of the J/ψ yield is due to decays of ψ' and χ_c mesons

Nuclear effects on the Parton Distribution Functions

The probability of finding a gluon with a momentum fraction x is *not* the same in a free proton as in a proton inside a nucleus; this “detail” has significant consequences

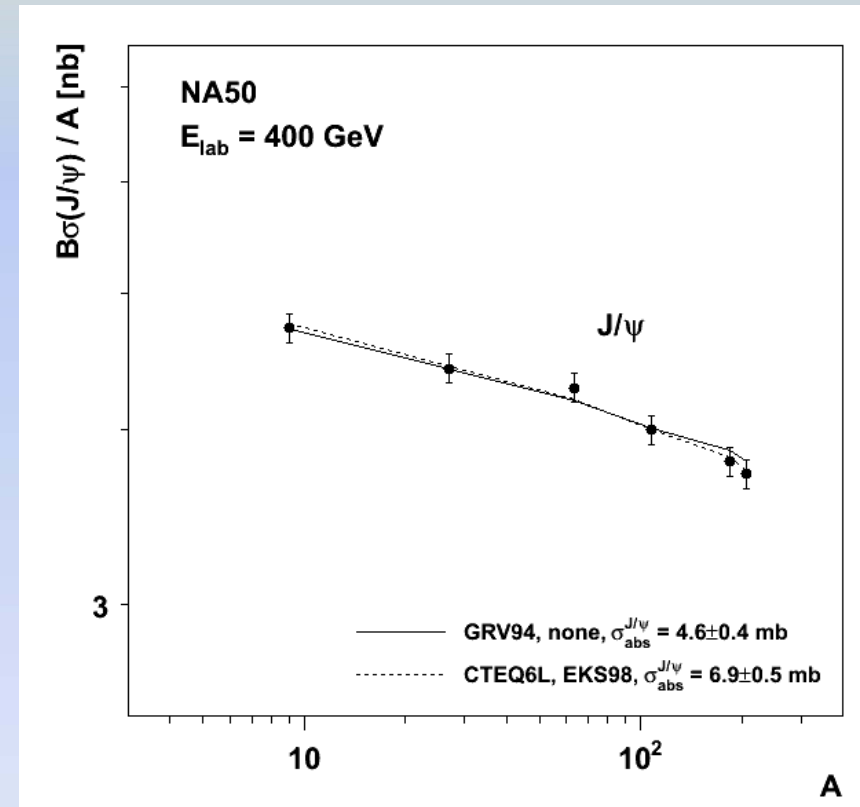
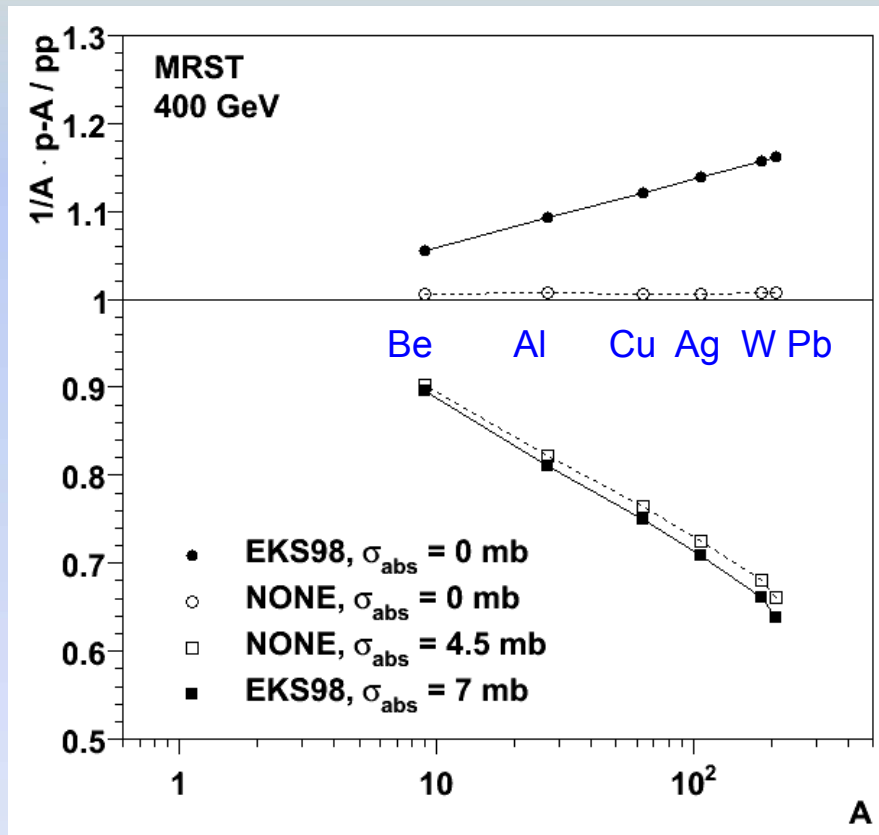


The existence of nuclear effects on the PDFs is well established but their *level* is not accurately known \Rightarrow calculations done with several models (EKS98, nDS, EPS09, etc)

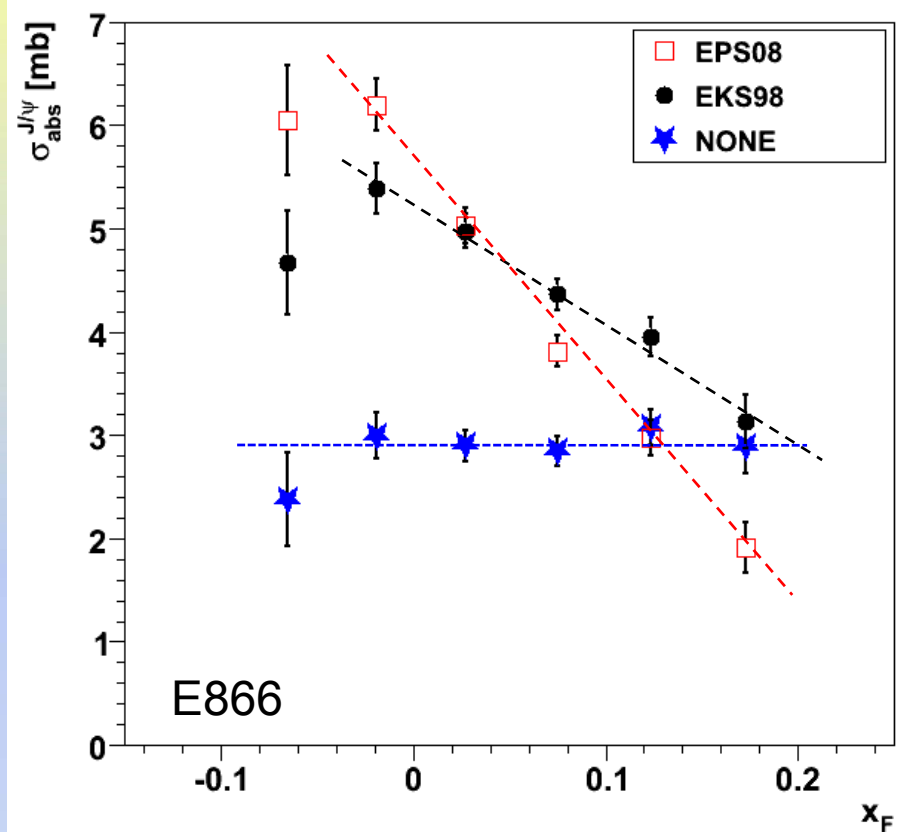
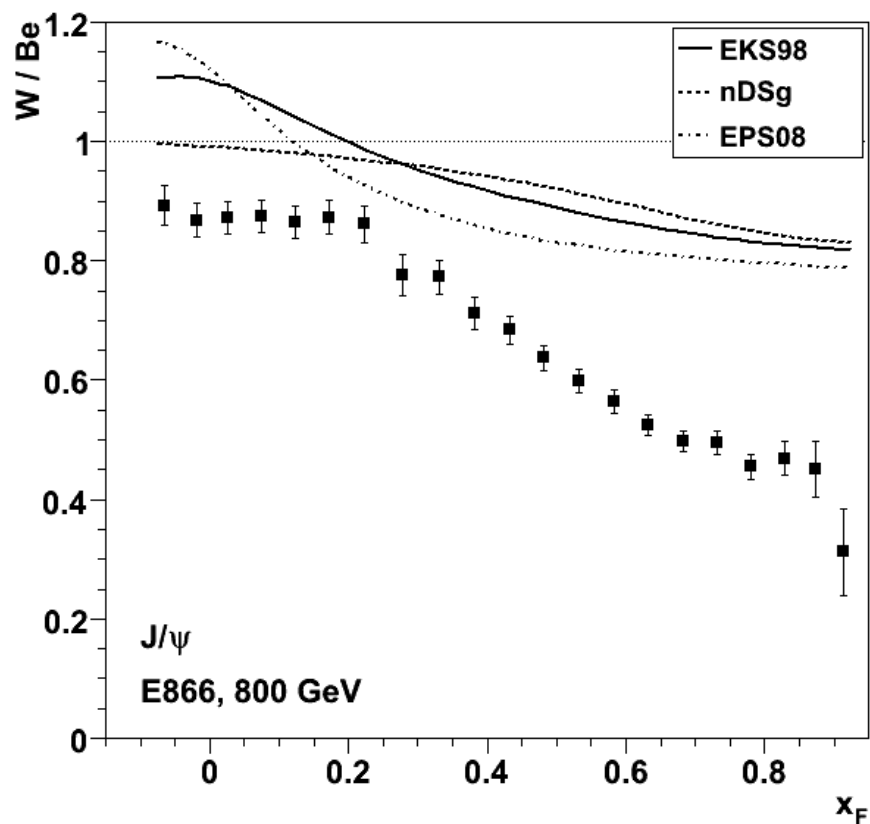
Nuclear effects on the PDFs vs. final state absorption

At x values ~ 0.1 – 0.4 (SPS energies), there is gluon *anti-shadowing* (EKS98); the J/ψ prod. cross section per nucleon *increases* from pp to p-Pb (before final state absorption)

\Rightarrow The NA50 measurements are equally well described using $\sigma_{\text{abs}} = 6.9$ mb (with EKS98) or $\sigma_{\text{abs}} = 4.6$ mb (with “free protons”)



J/ψ σ_{abs} versus x_F : the importance of the nPDFs



- The nuclear effects on the PDFs are a function of Bjorken- x
 \Rightarrow energy *and* x_F (or rapidity) dependent
- At $x_F < 0.2$: strong anti-shadowing in EKS98 and EPS08 :
 \Rightarrow In the absence of other effects, the E866 W/Be ratio should be higher than unity
- The nuclear modifications of the PDFs significantly change the x_F dependence of σ_{abs}

J/ψ nuclear dependence measurements: a global summary

The nuclear dependence of the J/ψ production cross section was studied by several experiments, probing different collision energies and J/ψ kinematics

Experiment	E_{lab} [GeV]	Collision systems	Phase space
NA3	200	p-H, Pt	$0.0 < x_F < 0.7$
NA50	400	p-Be, Al, Cu, Ag, W, Pb	$-0.425 < y_{\text{cms}} < 0.575$
NA50	450	p-Be, Al, Cu, Ag, W	$-0.50 < y_{\text{cms}} < 0.50$
E866	800	p-Be, W	$-0.10 < x_F < 0.93$
HERA-B	920	p-C, W	$-0.34 < x_F < 0.14$

Experiment	$\sqrt{s_{NN}}$ [GeV]	Collision systems	Phase space
PHENIX	200	pp, d-Au	$ y_{\text{cms}} < 0.35, 1.2 < y_{\text{cms}} < 2.2$

NA60 measured the J/ψ at 400 and 158 GeV (energy of the heavy-ion data) with a proton beam incident on 7 nuclear targets: Be, Al, Cu, In, W, Pb and U

$0.28 < y_{\text{cms}} < 0.78$ (158 GeV) and
 $-0.17 < y_{\text{cms}} < 0.33$ (400 GeV)

Results shown at QM09

J/ψ σ_{abs} for each kinematical window and nPDF set

Exp.	x_F	$\sigma_{\text{abs}}^{J/\psi}$ [mb]				
		NONE	nDS	nDSg	EKS98	EPS08
NA3	0.05	3.77 ± 0.98	3.94 ± 0.99	4.27 ± 1.00	5.79 ± 1.07	7.00 ± 1.12
	0.15	5.35 ± 0.88	5.46 ± 0.88	5.85 ± 0.89	7.38 ± 0.95	8.15 ± 0.98
	0.25	4.66 ± 0.98	4.63 ± 0.98	5.01 ± 0.99	6.18 ± 1.04	6.38 ± 1.05
	0.35	$4.96^{+1.51}_{-1.56}$	$4.71^{+1.49}_{-1.54}$	$5.07^{+1.51}_{-1.56}$	$5.81^{+1.56}_{-1.61}$	$5.62^{+1.55}_{-1.60}$
NA50-400		4.83 ± 0.63	4.74 ± 0.62	4.73 ± 0.62	7.01 ± 0.70	7.98 ± 0.74
450-LI		4.51 ± 1.58	4.39 ± 1.58	4.39 ± 1.58	6.89 ± 1.76	7.93 ± 1.83
450-HI		4.82 ± 1.10	4.71 ± 1.09	4.71 ± 1.09	7.17 ± 1.22	8.21 ± 1.28
E866	-0.0652	$2.37^{+0.83}_{-0.77}$	$2.32^{+0.83}_{-0.77}$	$3.01^{+0.85}_{-0.79}$	$4.67^{+0.92}_{-0.85}$	$6.06^{+0.98}_{-0.90}$
	-0.0188	$3.00^{+0.73}_{-0.69}$	$2.85^{+0.73}_{-0.69}$	$3.62^{+0.75}_{-0.71}$	$5.39^{+0.82}_{-0.76}$	$6.20^{+0.85}_{-0.79}$
	+0.0269	$2.90^{+0.71}_{-0.67}$	$2.65^{+0.70}_{-0.66}$	$3.27^{+0.72}_{-0.68}$	$4.98^{+0.78}_{-0.73}$	$5.03^{+0.78}_{-0.73}$
	+0.0747	$2.85^{+0.71}_{-0.67}$	$2.50^{+0.70}_{-0.66}$	$2.65^{+0.70}_{-0.66}$	$4.36^{+0.76}_{-0.71}$	$3.81^{+0.74}_{-0.70}$
	+0.1235	$3.07^{+0.72}_{-0.68}$	$2.61^{+0.71}_{-0.67}$	$2.13^{+0.69}_{-0.65}$	$3.95^{+0.75}_{-0.71}$	$2.98^{+0.72}_{-0.68}$
	+0.1729	$2.89^{+0.74}_{-0.70}$	$2.31^{+0.73}_{-0.68}$	$1.28^{+0.69}_{-0.65}$	$3.13^{+0.75}_{-0.71}$	$1.91^{+0.71}_{-0.67}$
HERA-B	-0.158	—	—	—	$0.73^{+1.42}_{-0.73}$	$2.23^{+1.52}_{-1.35}$
	-0.118	$0.34^{+1.22}_{-0.34}$	$0.42^{+1.22}_{-0.42}$	$0.96^{+1.25}_{-0.96}$	$2.34^{+1.33}_{-1.20}$	$3.88^{+1.43}_{-1.28}$
	-0.079	$1.39^{+1.18}_{-1.08}$	$1.38^{+1.18}_{-1.08}$	$2.04^{+1.22}_{-1.11}$	$3.68^{+1.32}_{-1.19}$	$5.08^{+1.41}_{-1.26}$
	-0.040	$2.11^{+1.21}_{-1.10}$	$1.99^{+1.20}_{-1.09}$	$2.76^{+1.24}_{-1.13}$	$4.53^{+1.36}_{-1.22}$	$5.46^{+1.42}_{-1.27}$
	-0.002	$2.10^{+1.28}_{-1.15}$	$1.85^{+1.26}_{-1.14}$	$2.58^{+1.31}_{-1.18}$	$4.32^{+1.42}_{-1.27}$	$4.58^{+1.44}_{-1.29}$
	+0.037	$2.46^{+1.51}_{-1.34}$	$2.09^{+1.49}_{-1.32}$	$2.51^{+1.52}_{-1.35}$	$4.28^{+1.65}_{-1.45}$	$3.94^{+1.63}_{-1.43}$
	+0.075	$3.52^{+2.43}_{-2.02}$	$2.96^{+2.36}_{-1.97}$	$2.52^{+2.31}_{-1.93}$	$4.58^{+2.56}_{-2.11}$	$3.59^{+2.44}_{-2.02}$

Errors include the global systematic uncertainties of the ratios:

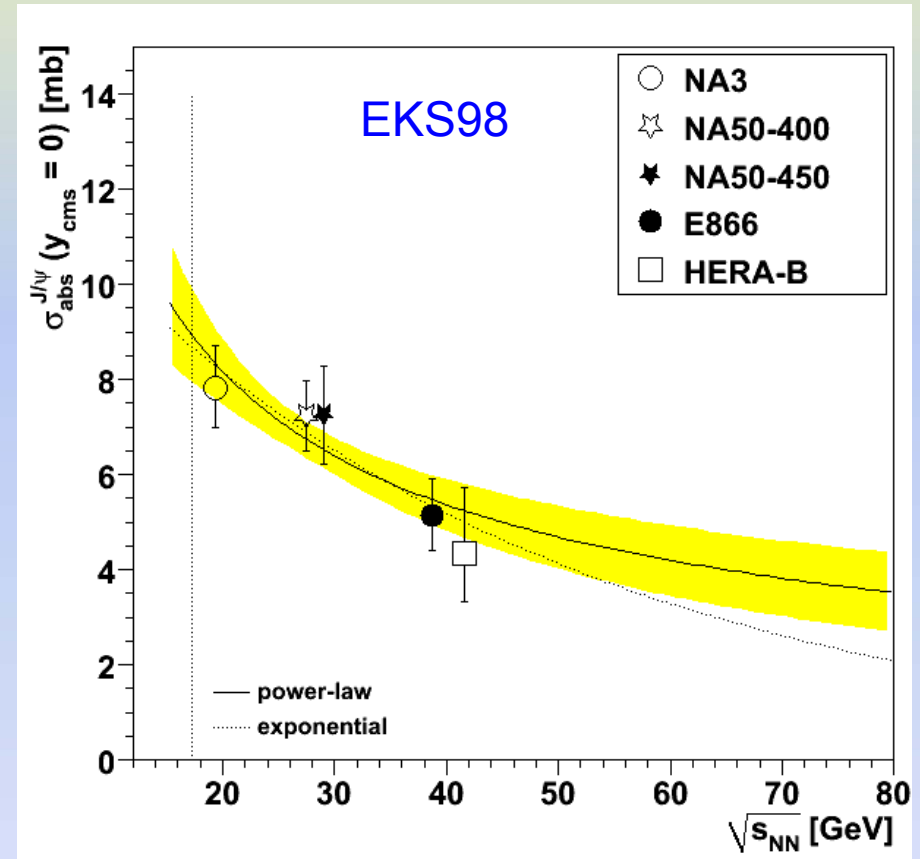
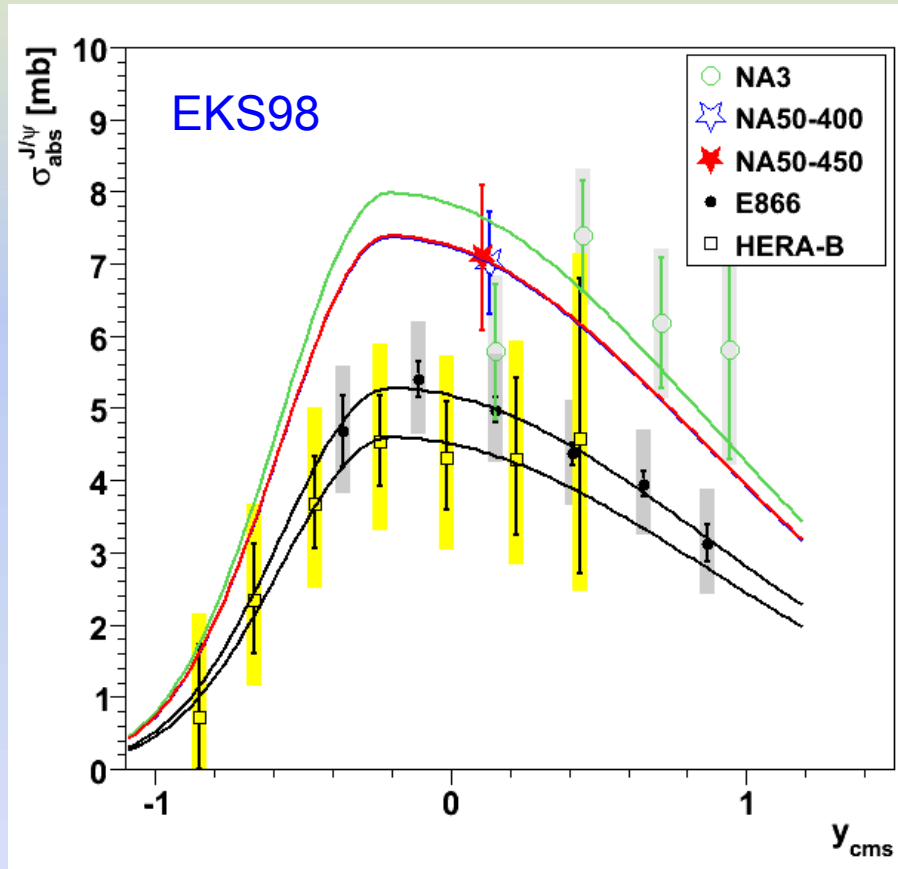
3% in NA3
3% in E866
4% in HERA-B

C. Lourenço, R. Vogt
and H.K. Wöhri,
JHEP 2 (09) 14

J/ψ σ_{abs} versus rapidity and collision energy

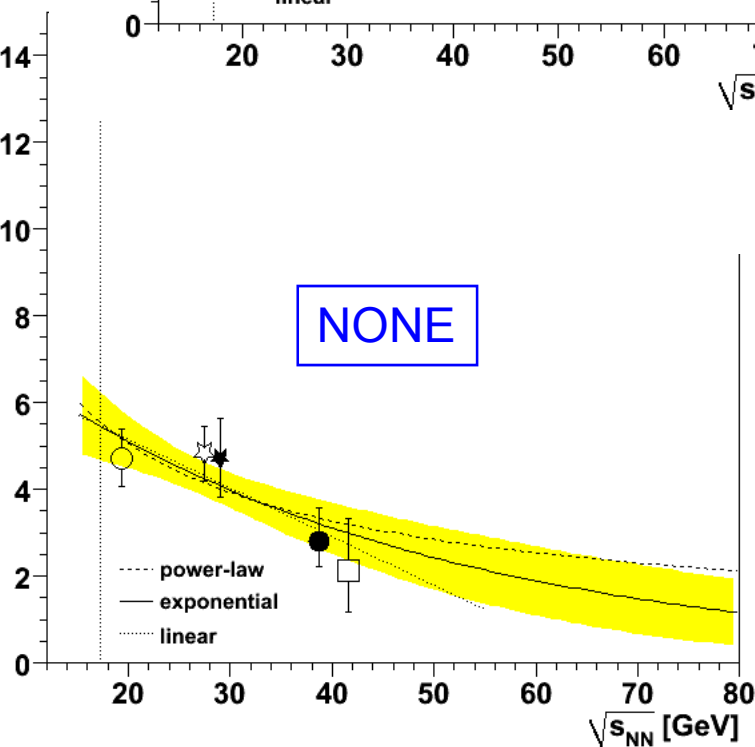
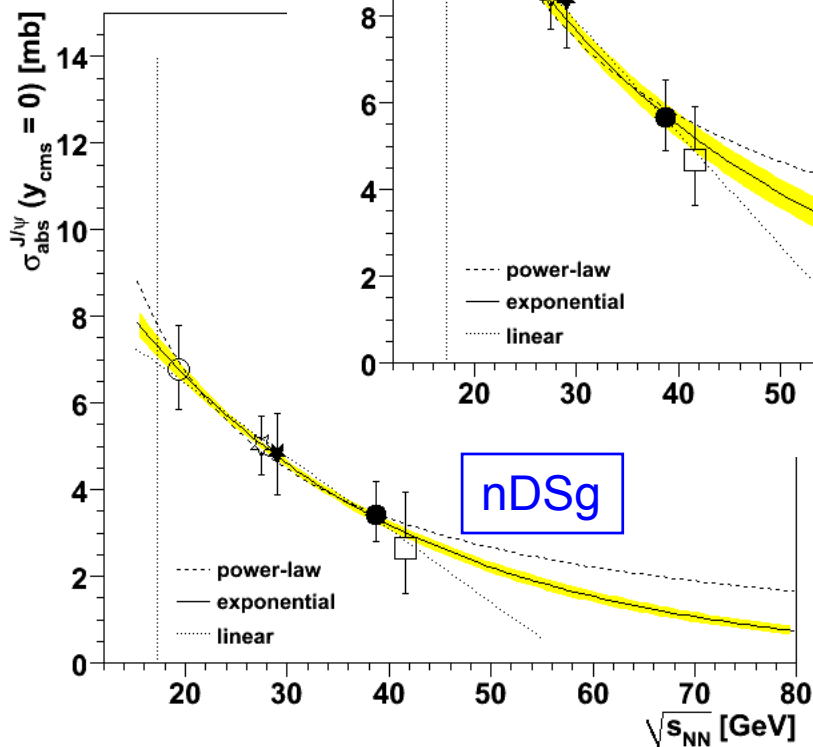
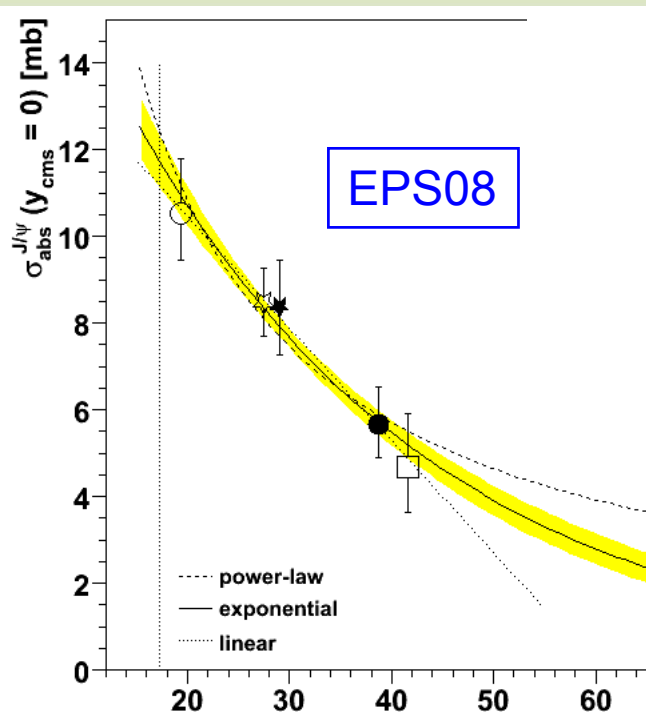
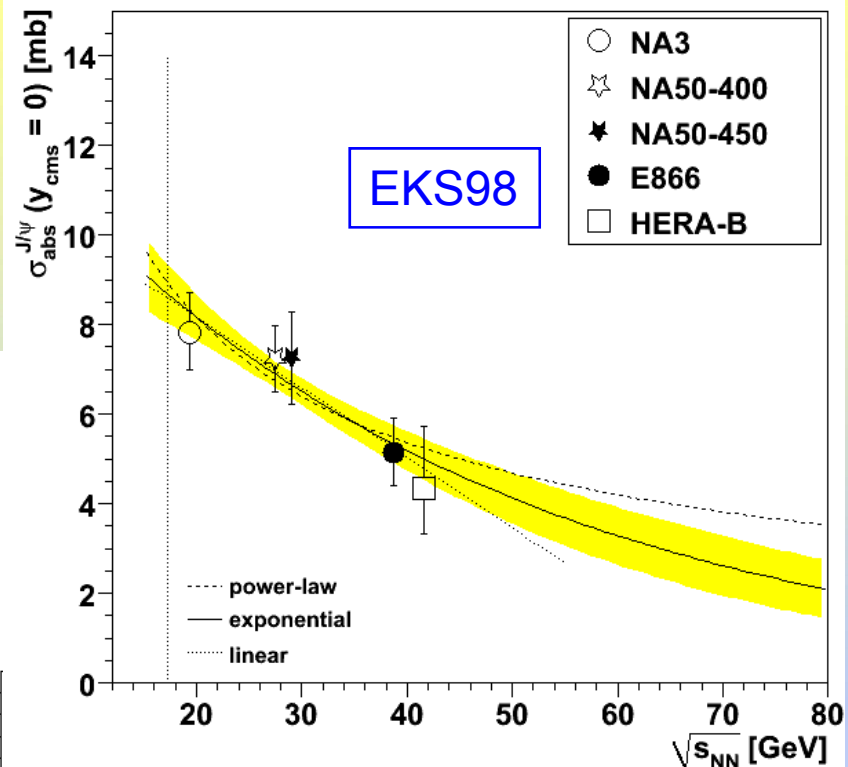
The E866 and HERA-B patterns have enough (accurate) points to define the *shape* of the rapidity dependence of σ_{abs}

σ_{abs} at $y_{\text{cms}}=0$ decreases with NN collision energy

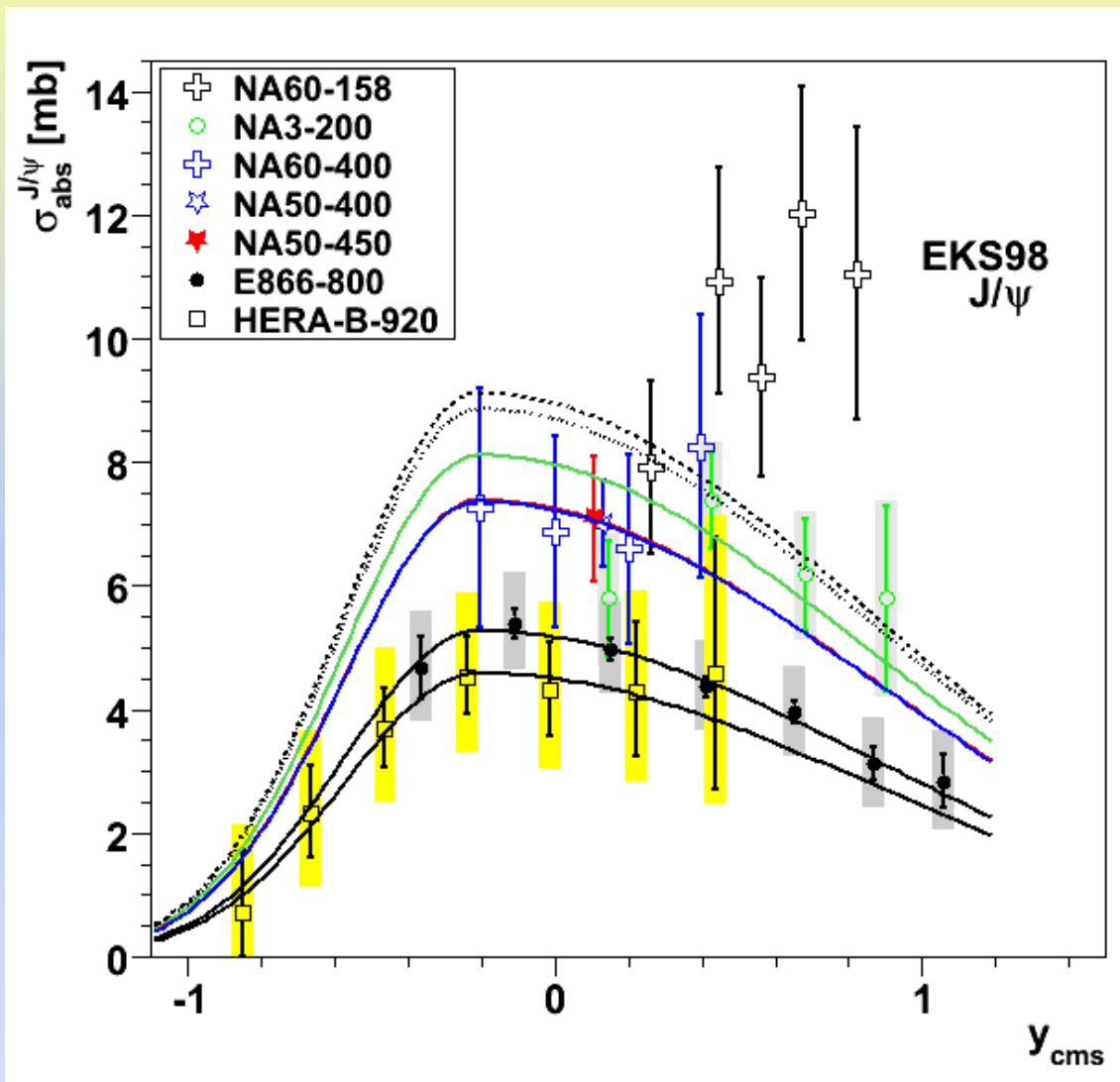


J/ψ σ_{abs} at $y_{\text{cms}}=0$ vs. $\sqrt{s_{\text{NN}}}$

Whatever nPDF model we use, σ_{abs} at $y_{\text{cms}}=0$ decreases with NN collision energy



What can we learn from the new NA60 data?



Extrapolation to $y_{\text{CMS}}=0$ at 158 GeV gives a σ_{abs} of:
 9.0 ± 0.9 mb with power-law
 8.7 ± 0.6 mb with exponential

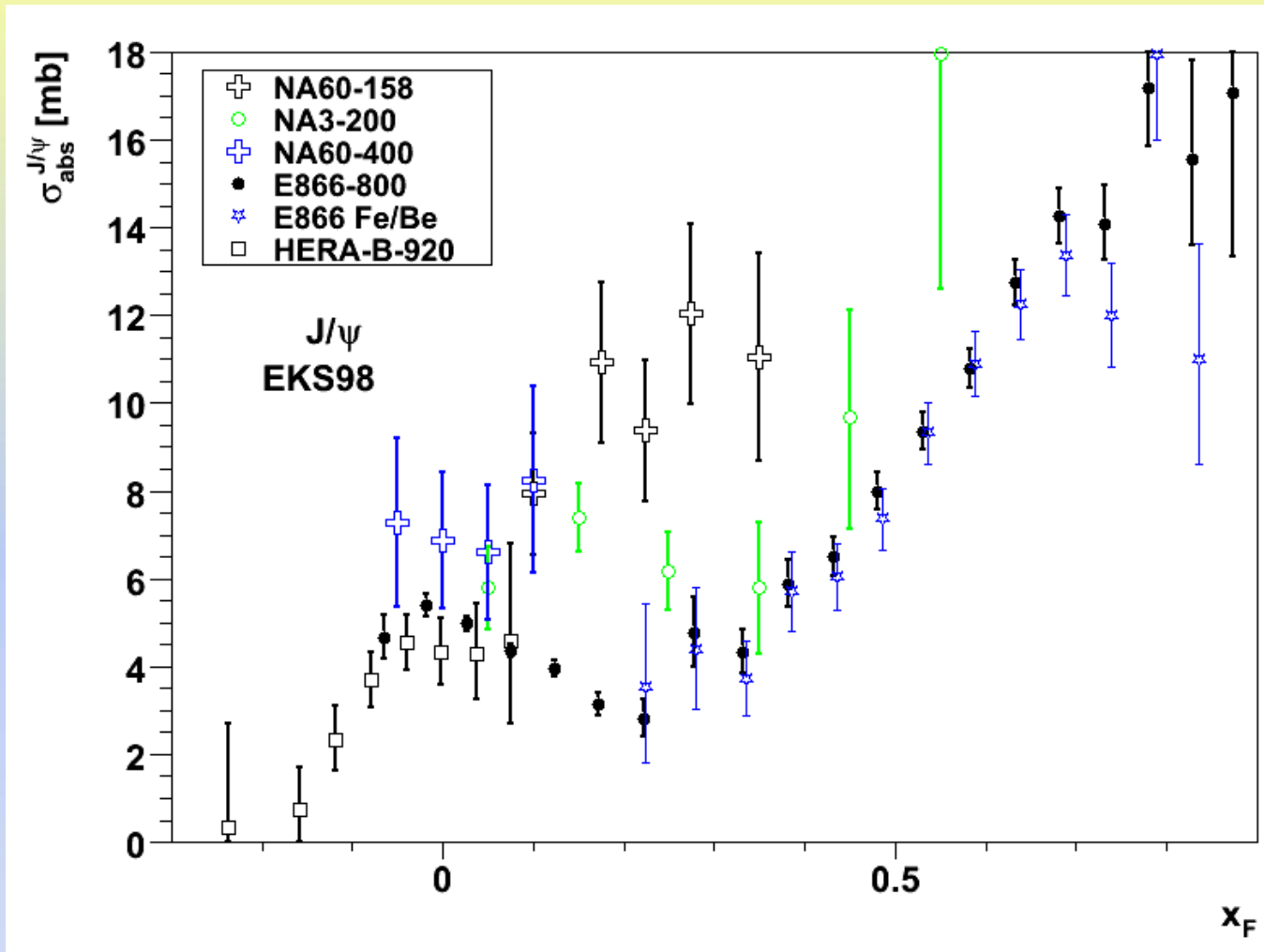
Let's compare to the new NA60 data, shown at QM09

The 400 GeV data points are perfectly compatible with the previously established trend

The first 158 GeV point sits on the expected curve but the others are much higher

Do we see a departure from the absorption pattern?
What about other nuclear matter effects?

The forward x_F region is visibly different



E866 shows that at forward x_F other effects play a role

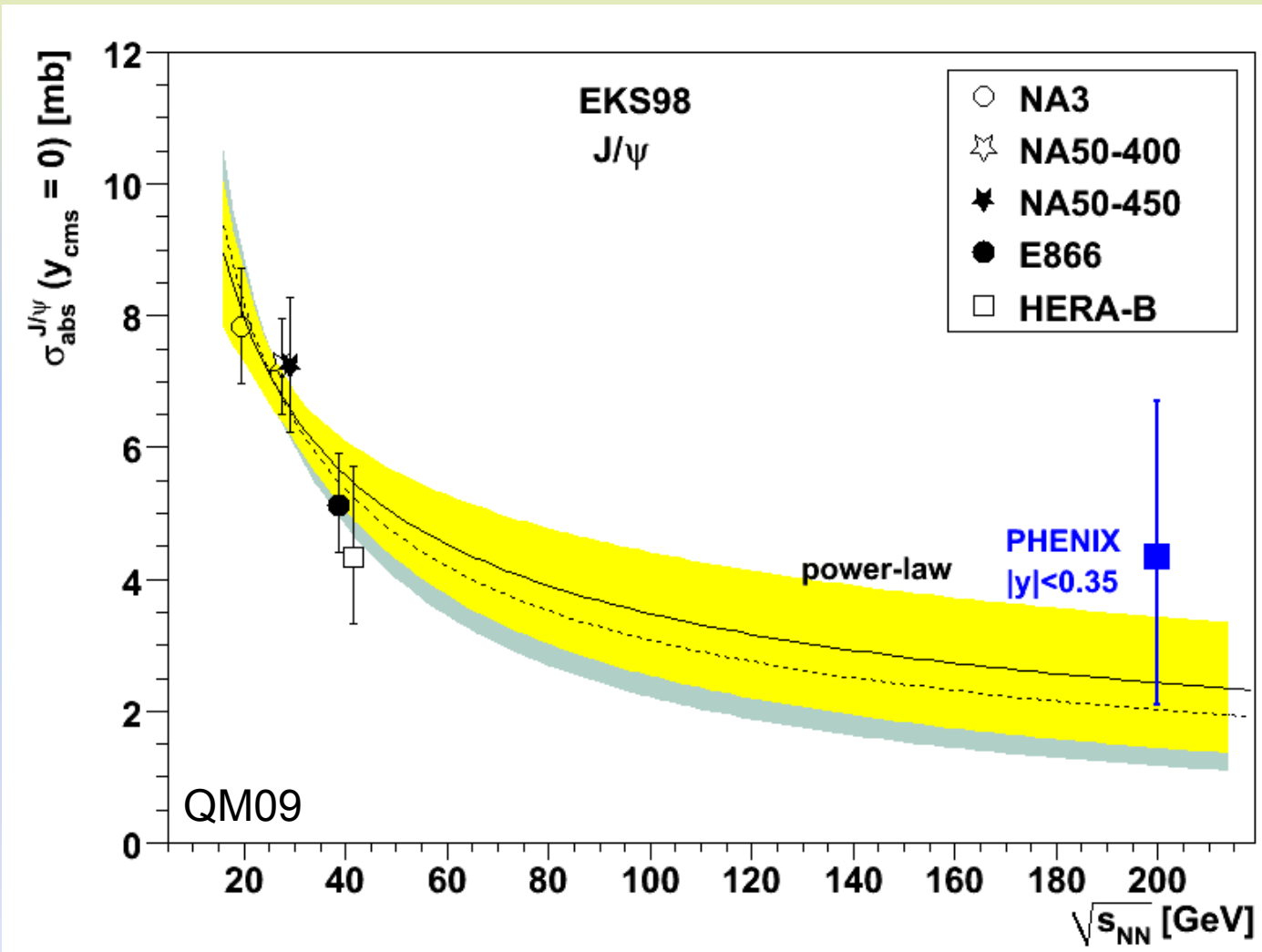
NA3 also shows much larger σ_{abs} at forward x_F

NA60-400 (at $x_F \sim 0$) is compatible with absorption only...

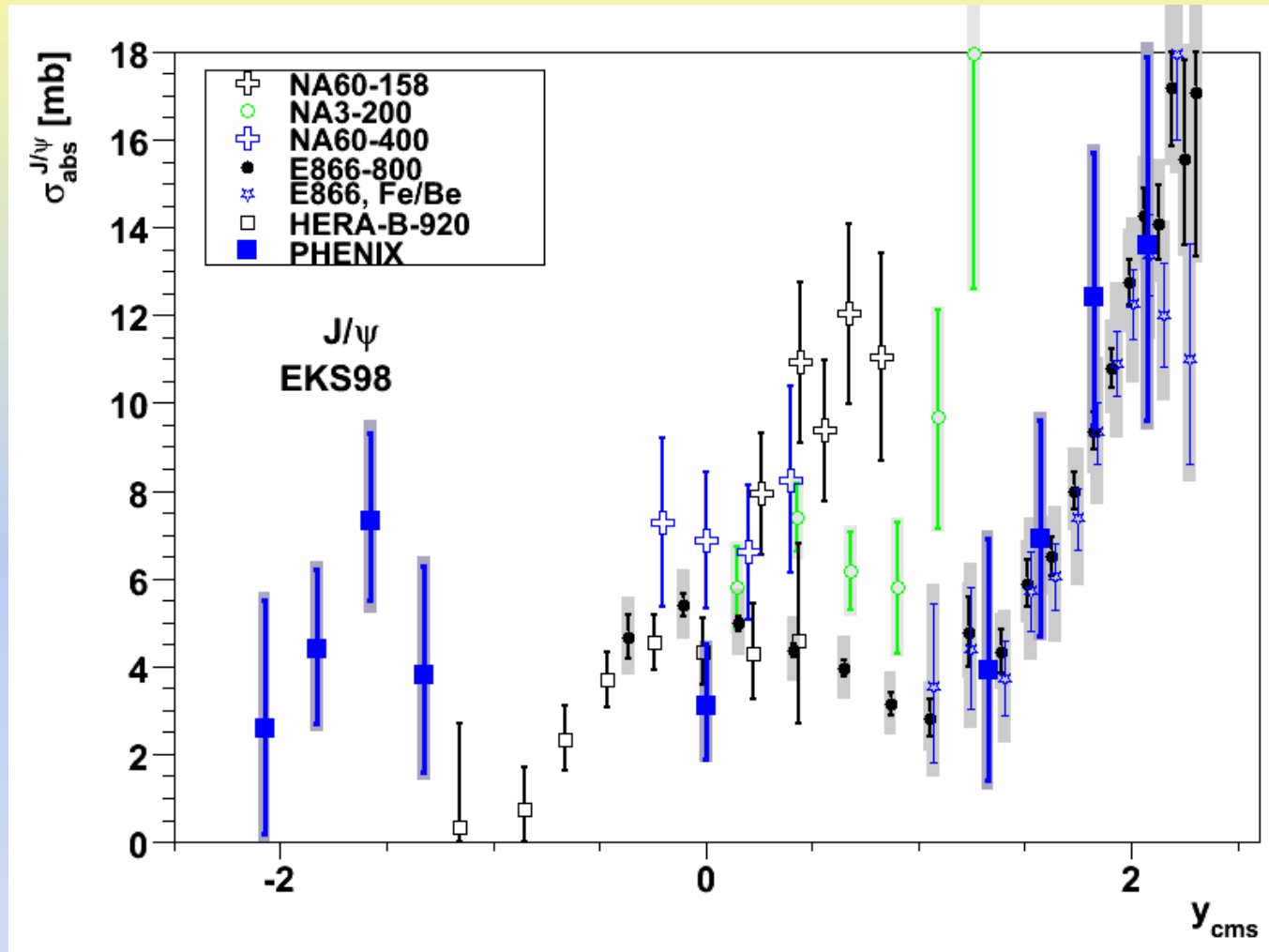
while the (forward) 158 GeV data seem to follow the E866 trend

How does PHENIX fit into the game?

The mid-rapidity PHENIX value is perfectly compatible with the power-law trend suggested by the fixed-target data

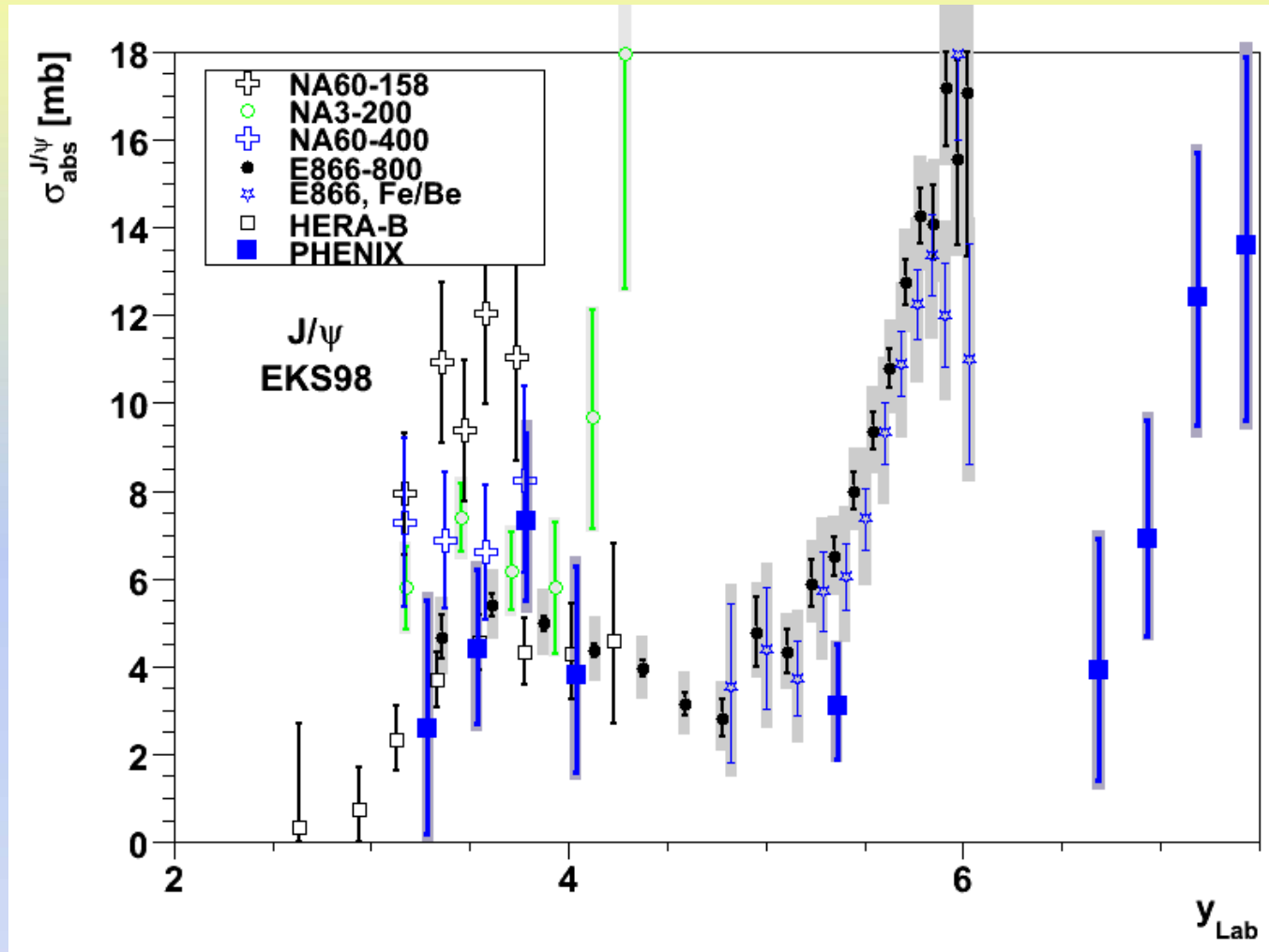


What can we learn from the PHENIX data?



The broad rapidity coverage of the PHENIX data should considerably help in discriminating the different cold nuclear effects, by comparing data sets as a function of several kinematical variables

What can we learn from the PHENIX data?



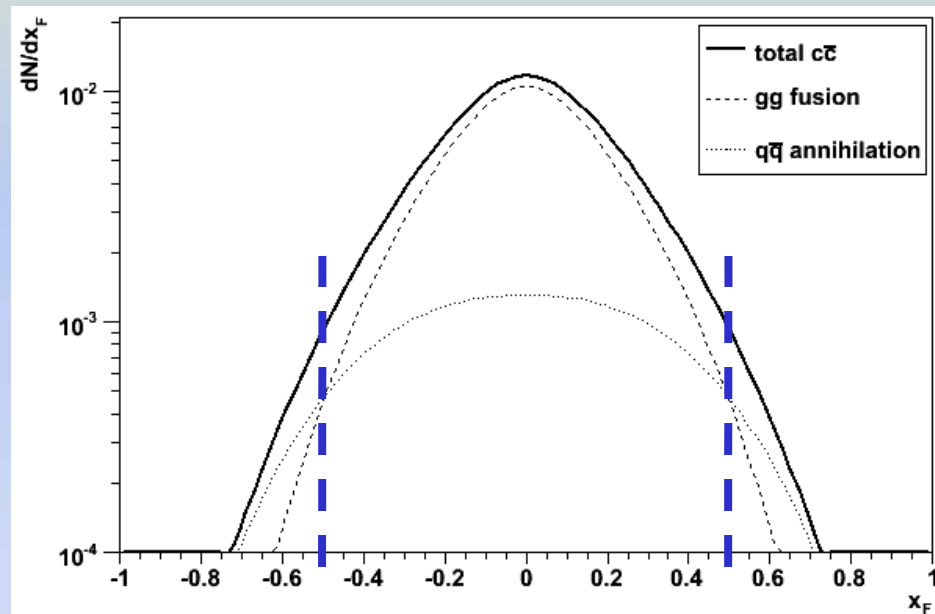
Unfortunately, the error bars are still very large

A first and simple look at parton energy loss

The beam partons may lose energy by traversing the nucleus, before J/ψ creation. We model this effect in a very simple way, assuming a constant fractional loss of energy per “collision”, $x_1' = x_1 (1 - \varepsilon_g)^{(N_{\text{coll}} - 1)}$, with the average N_{coll} from Glauber

The gluon and quark **energy loss** parameters are related by $\varepsilon_g = 9/4 \varepsilon_q$

Note: $q\bar{q}$ annihilation dominates quarkonium production for $x_F > 0.5$, according to the CEM and using CTEQ6L PDFs

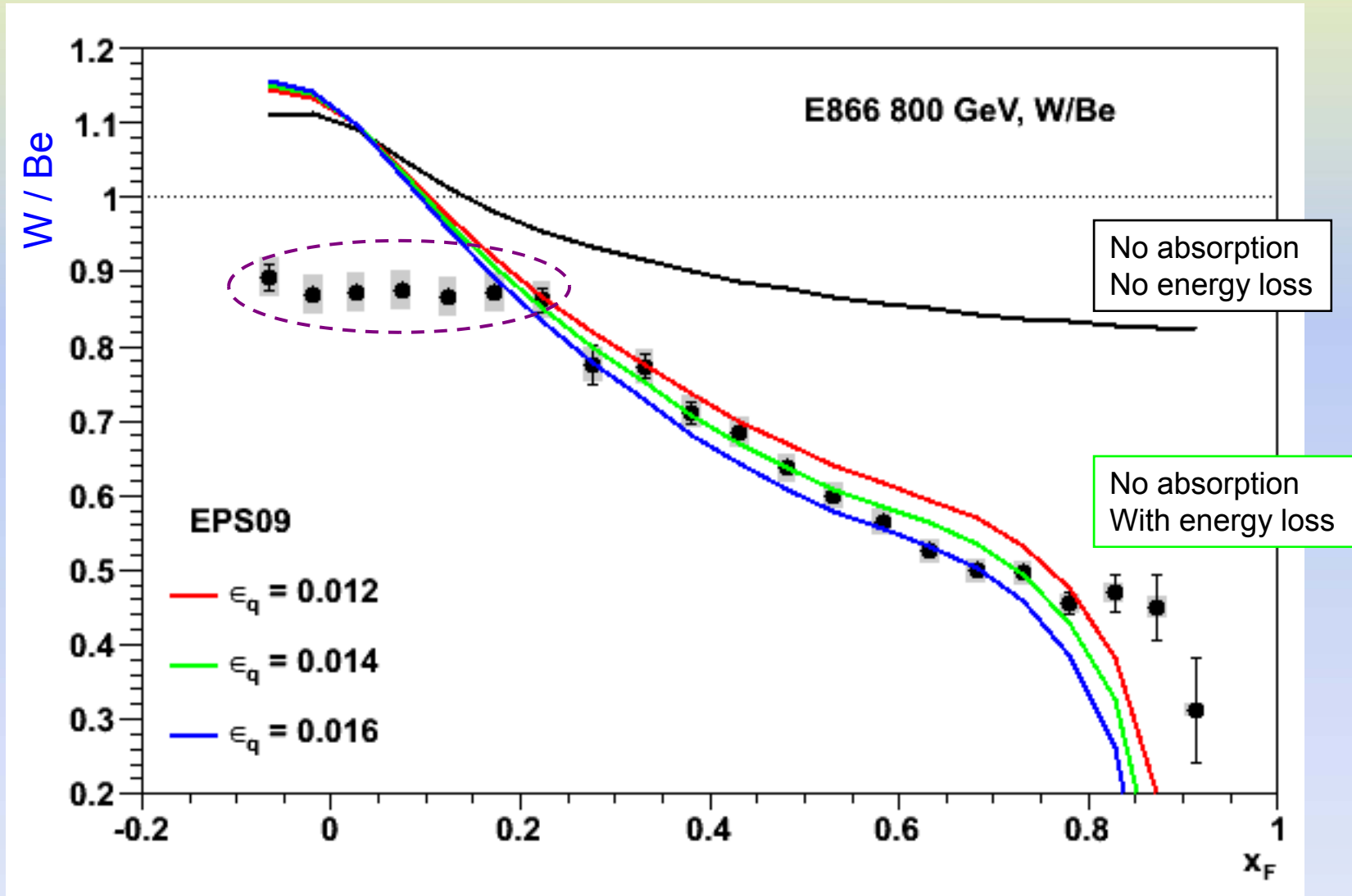


The **decreased energy** ($x_1' < x_1$) leads to a “**backward shift**” of the J/ψ ’s x_F distribution ($\rightarrow x_F' < x_F$)

E866, 800 GeV, p-W / p-Be ratio

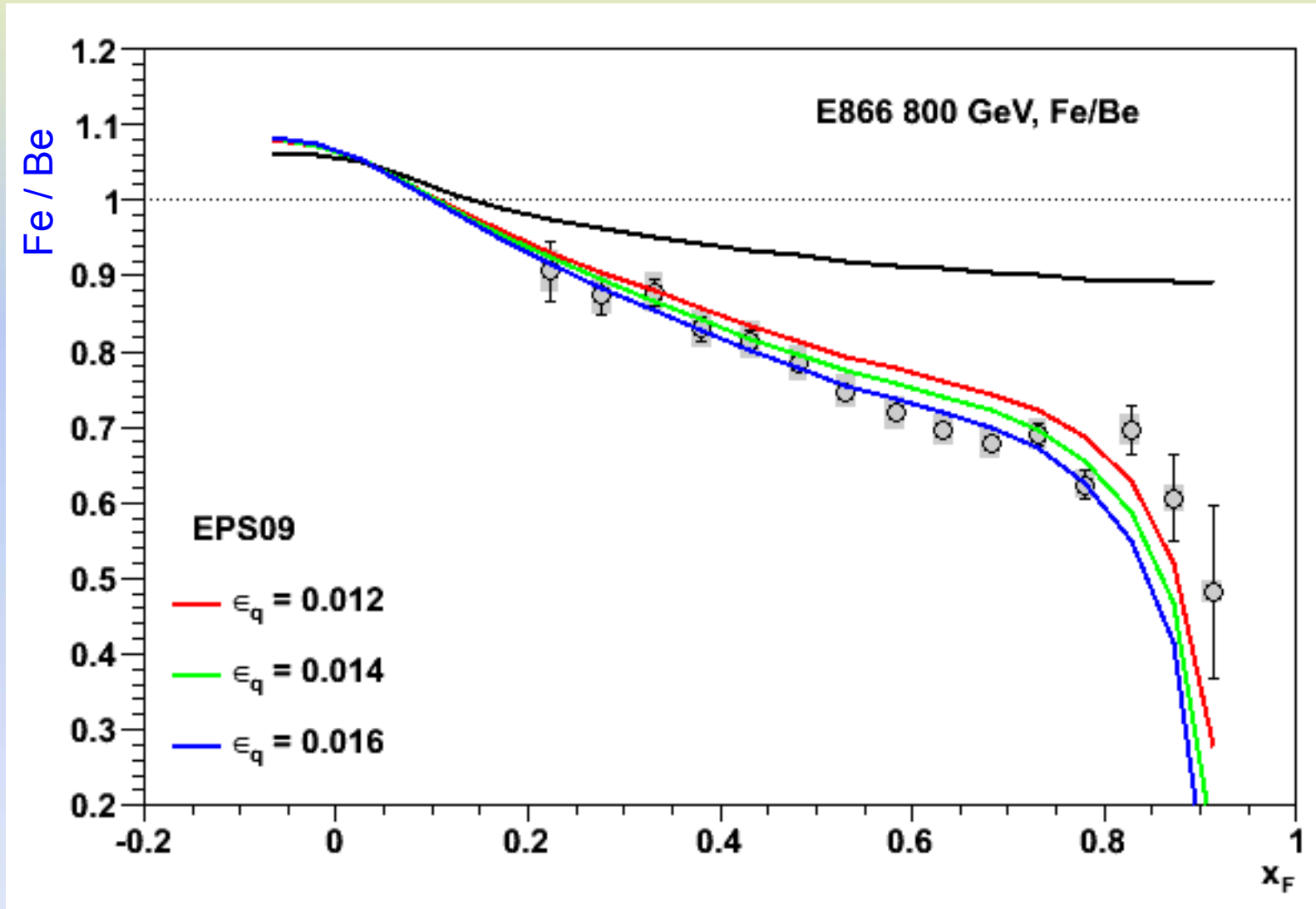
The $x_F < 0.2$ region is affected by final state absorption, not included in these curves

The $0.2 < x_F < 0.75$ window is well described by $\epsilon_q \sim 1.5\%$ and $\epsilon_g = 9/4 \epsilon_q \sim 3.3\%$



E866, 800 GeV, p-Fe / p-Be ratio

The p-Fe data of E866 is equally well reproduced with the same ϵ_q and ϵ_g values

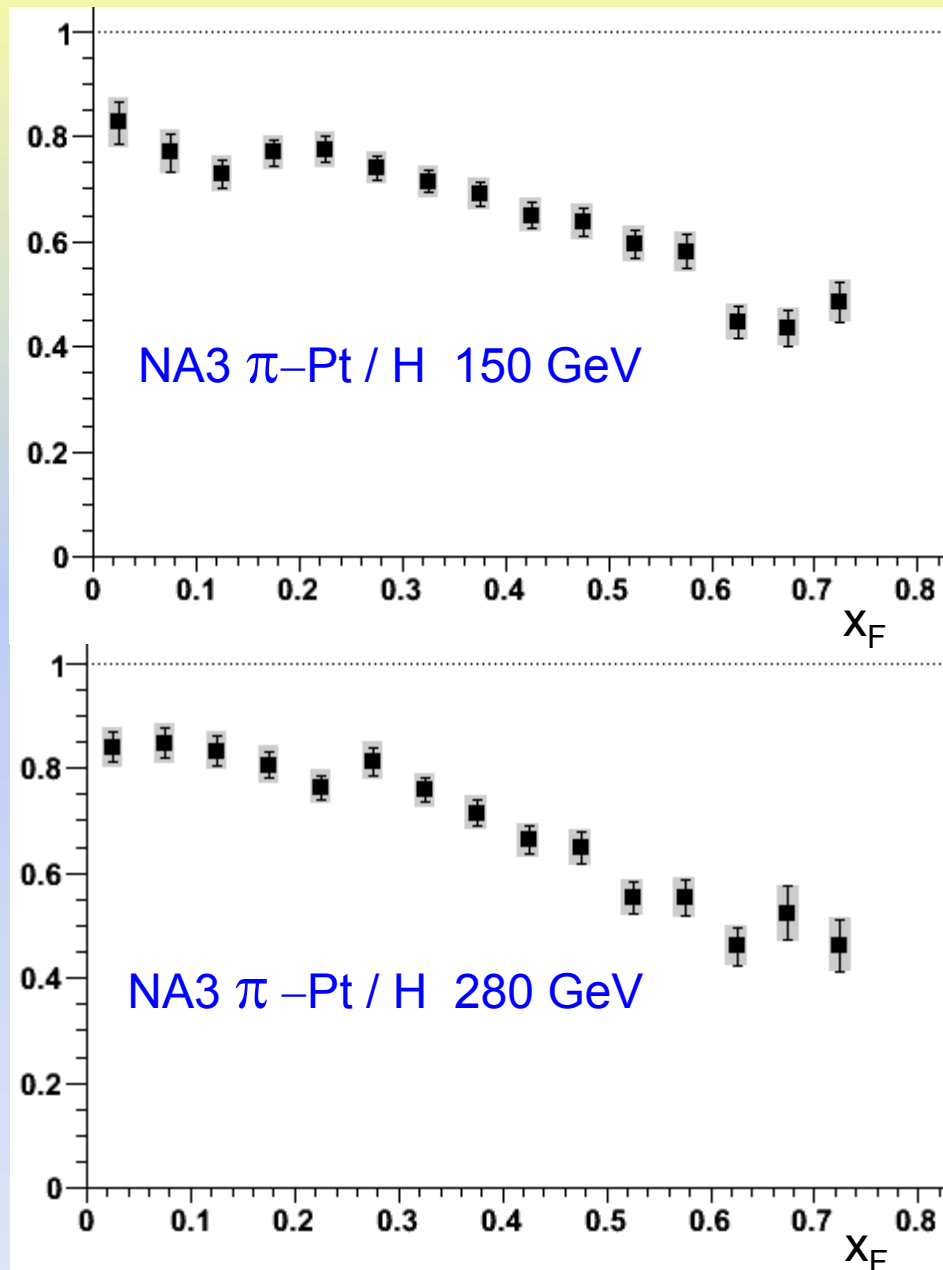
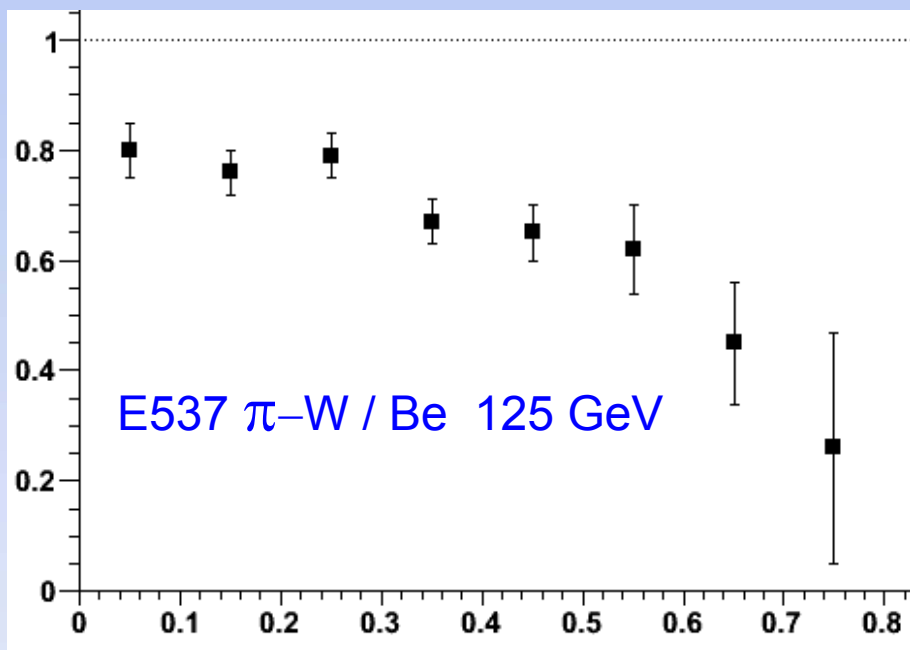


Future “ingredients” to settle the energy loss process

There are forward x_F J/ψ data from E866 (p-Fe,W), NA3 (p-Pt) and PHENIX (d-Au)

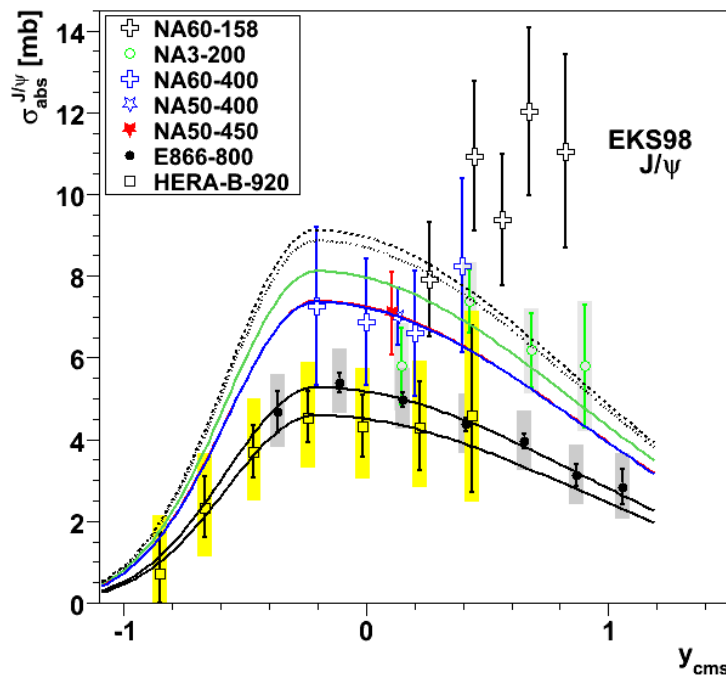
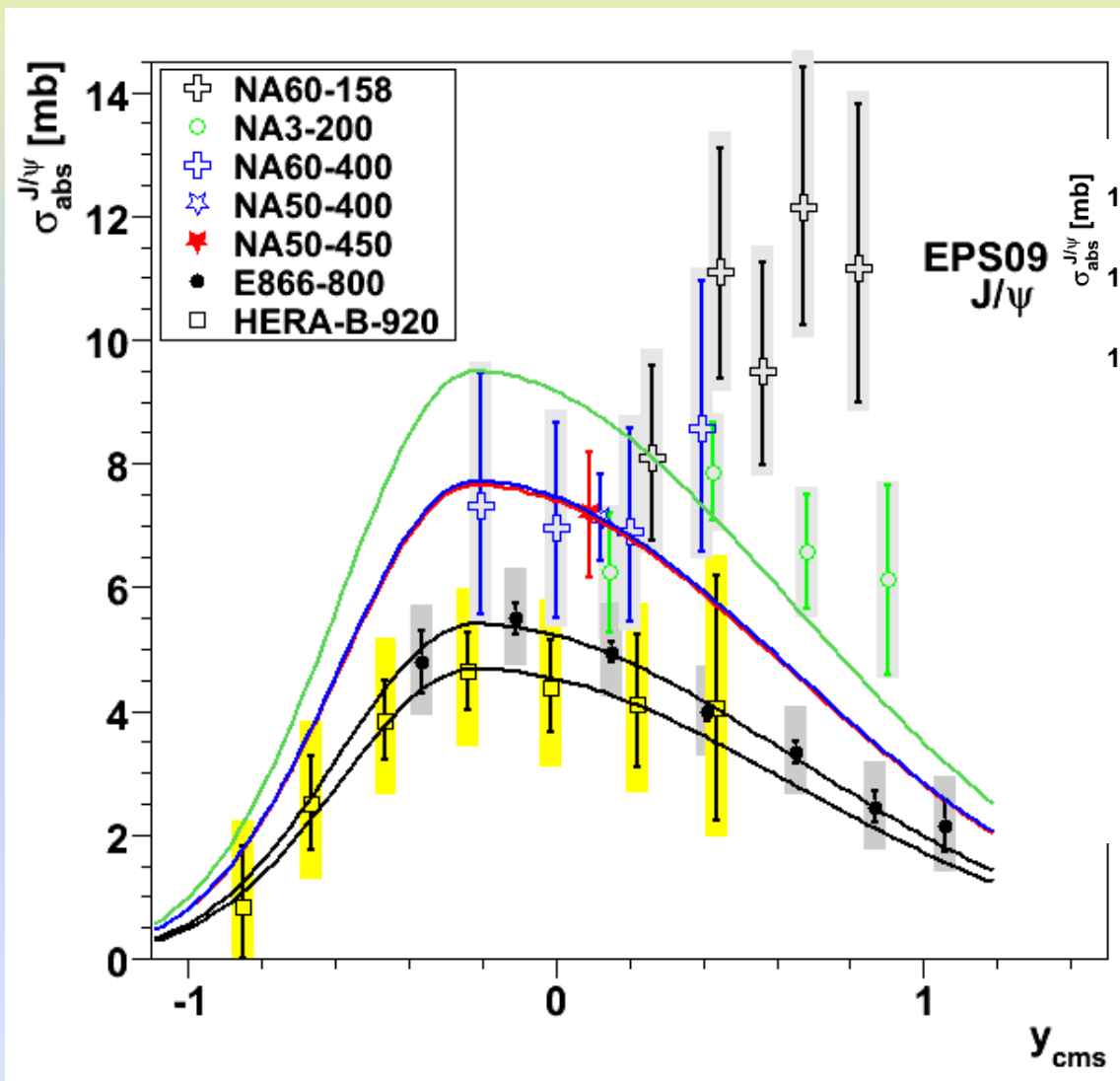
Plus the new open charm data of E866

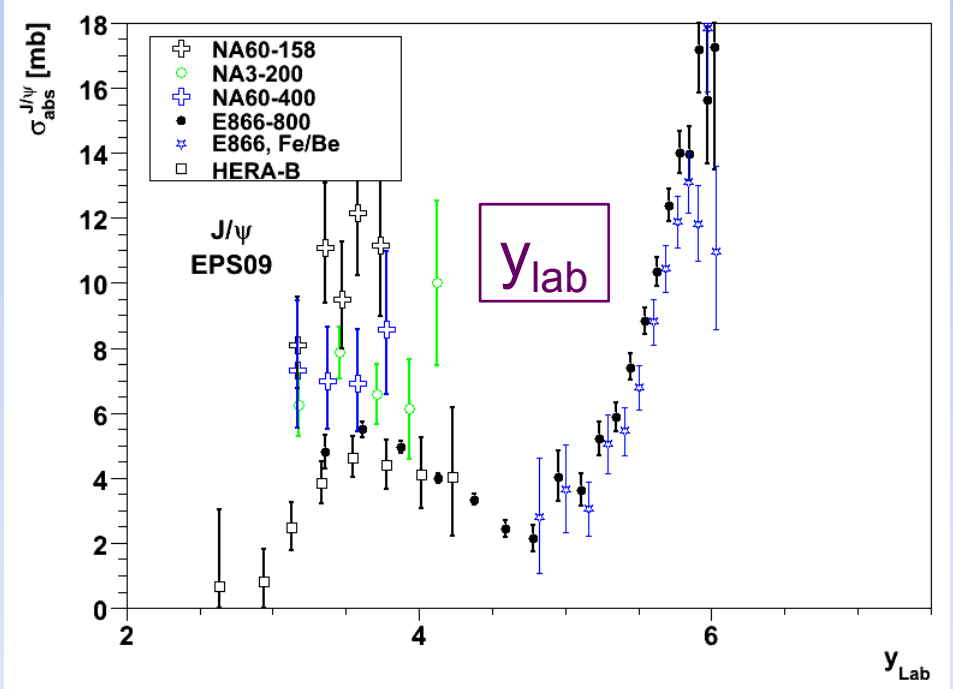
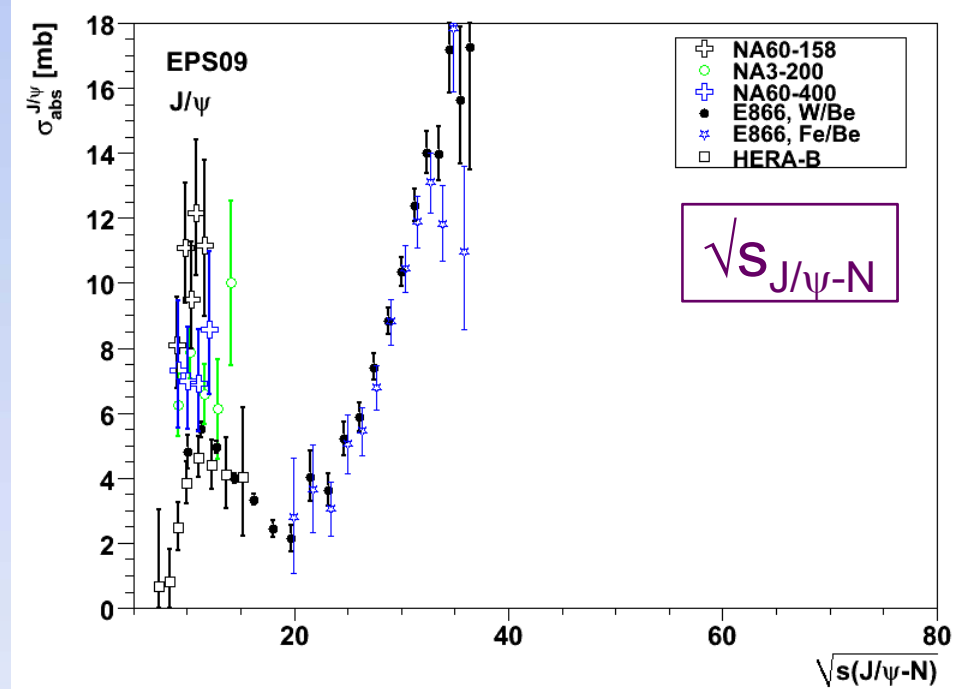
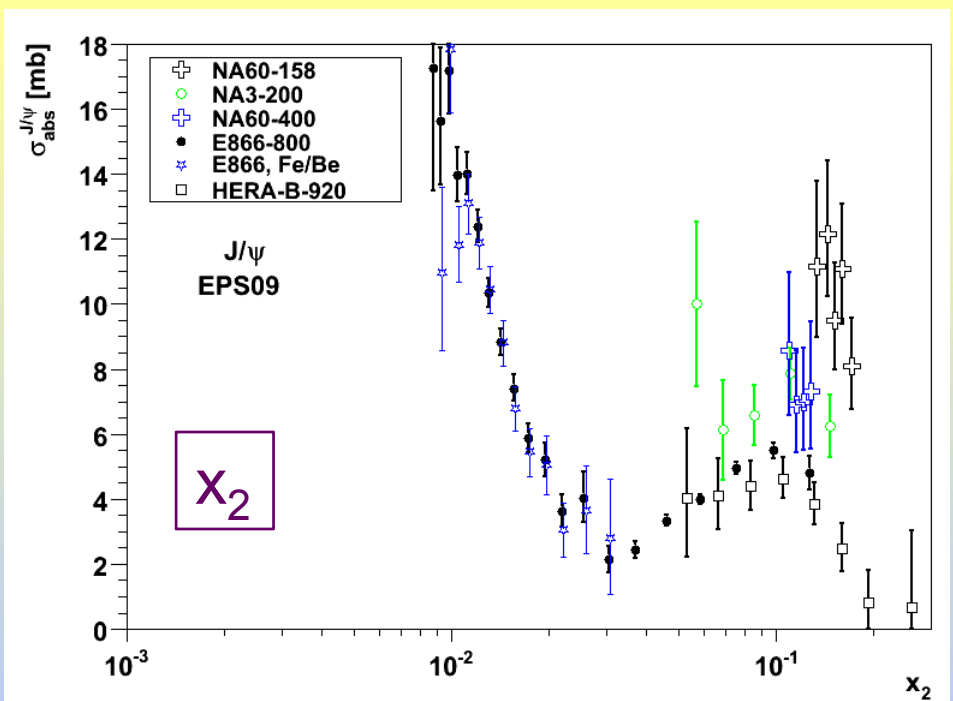
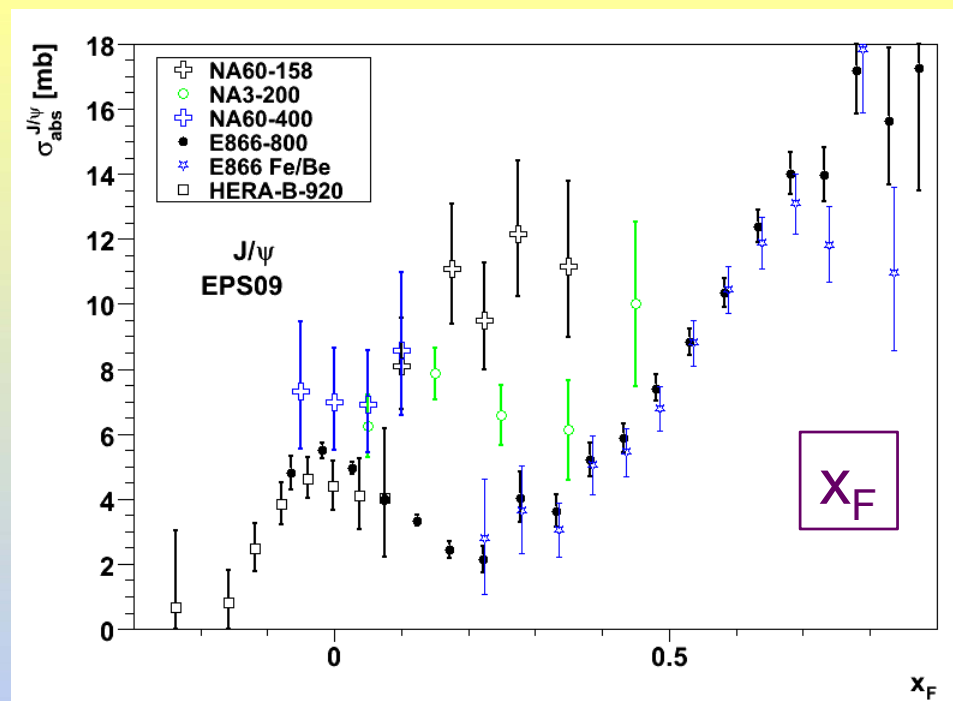
And Drell-Yan and π -A data which might help studying the quark energy loss



Recent progress using the EPS09 nPDFs

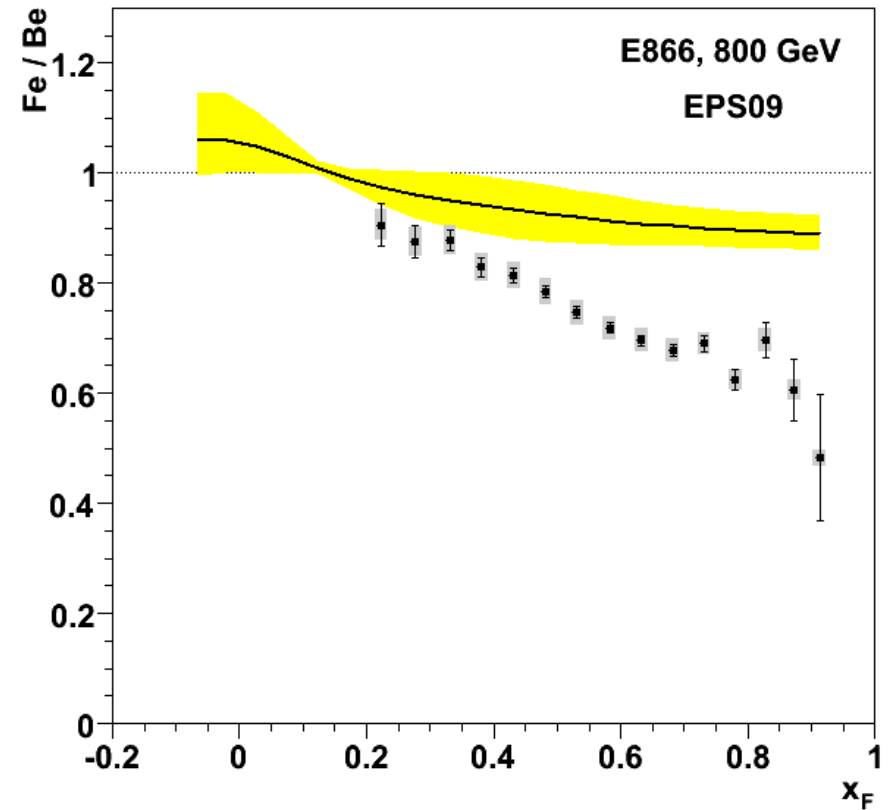
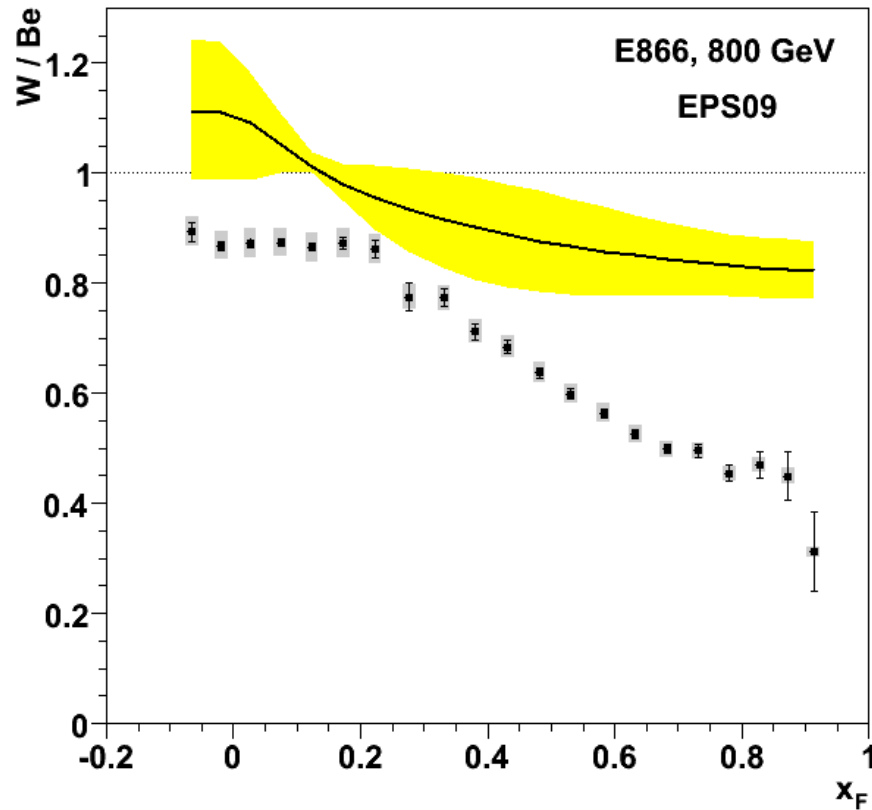
Here in Seattle, we have redone several figures using the EPS09 nPDFs



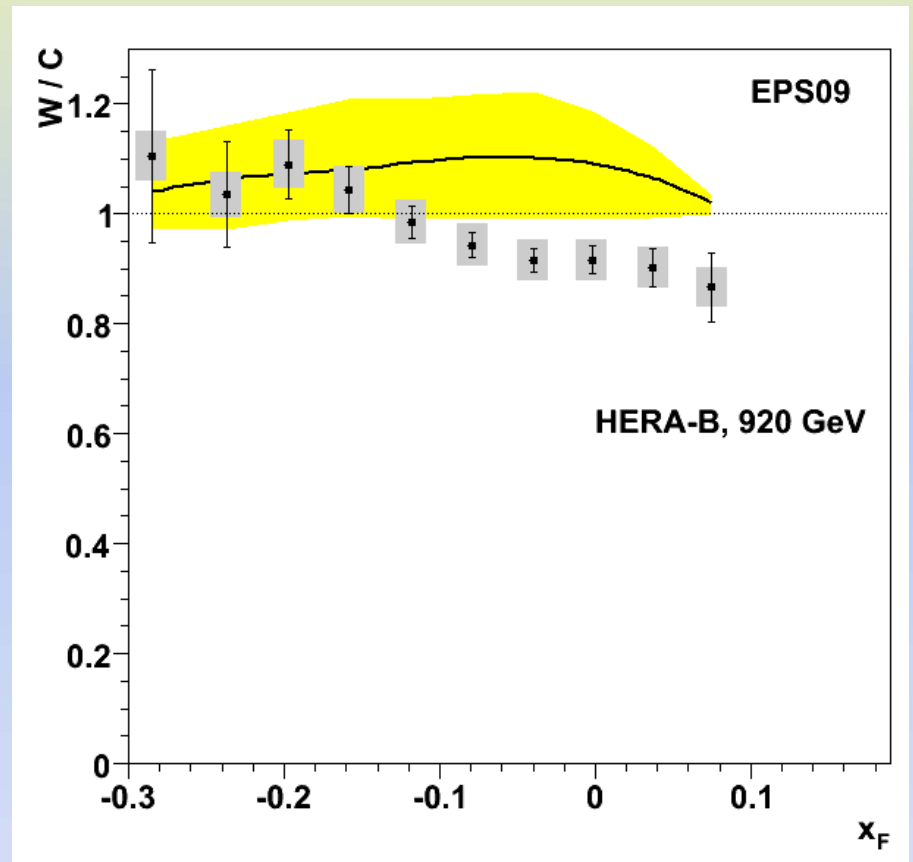
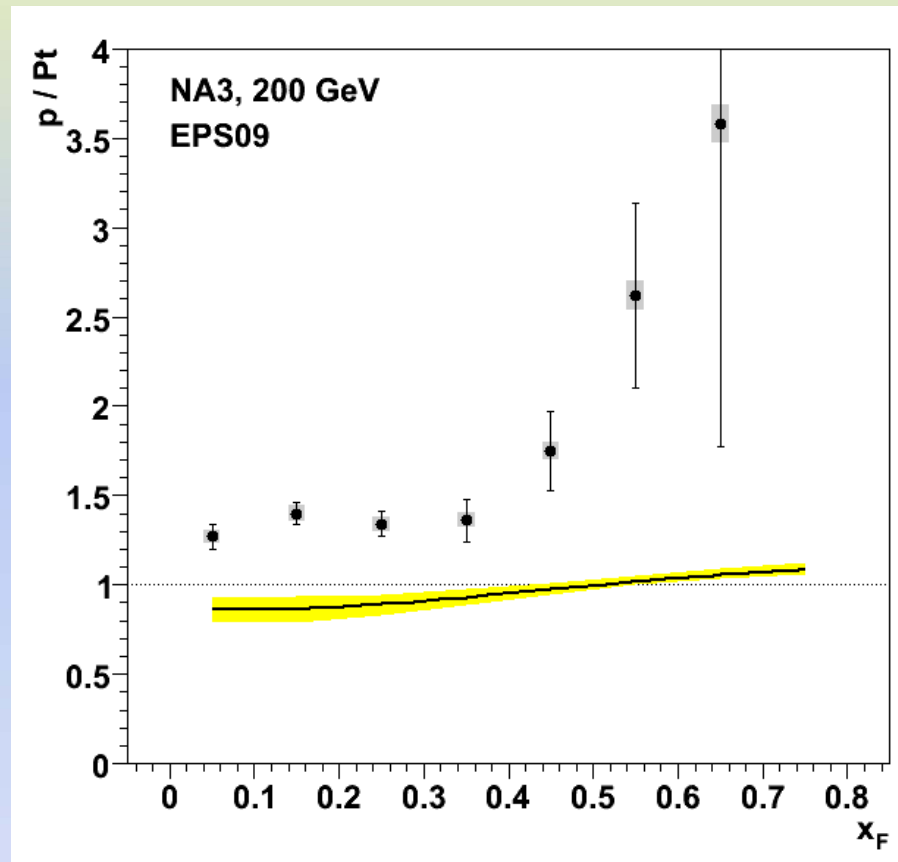


EPS09 uncertainty: E866 cases

- Uncertainty band calculated following the procedure outlined in the EPS09 paper [JHEP04(2009)065]
- It represents the sum in quadrature of 15 parameters changed by $\pm 1\sigma$

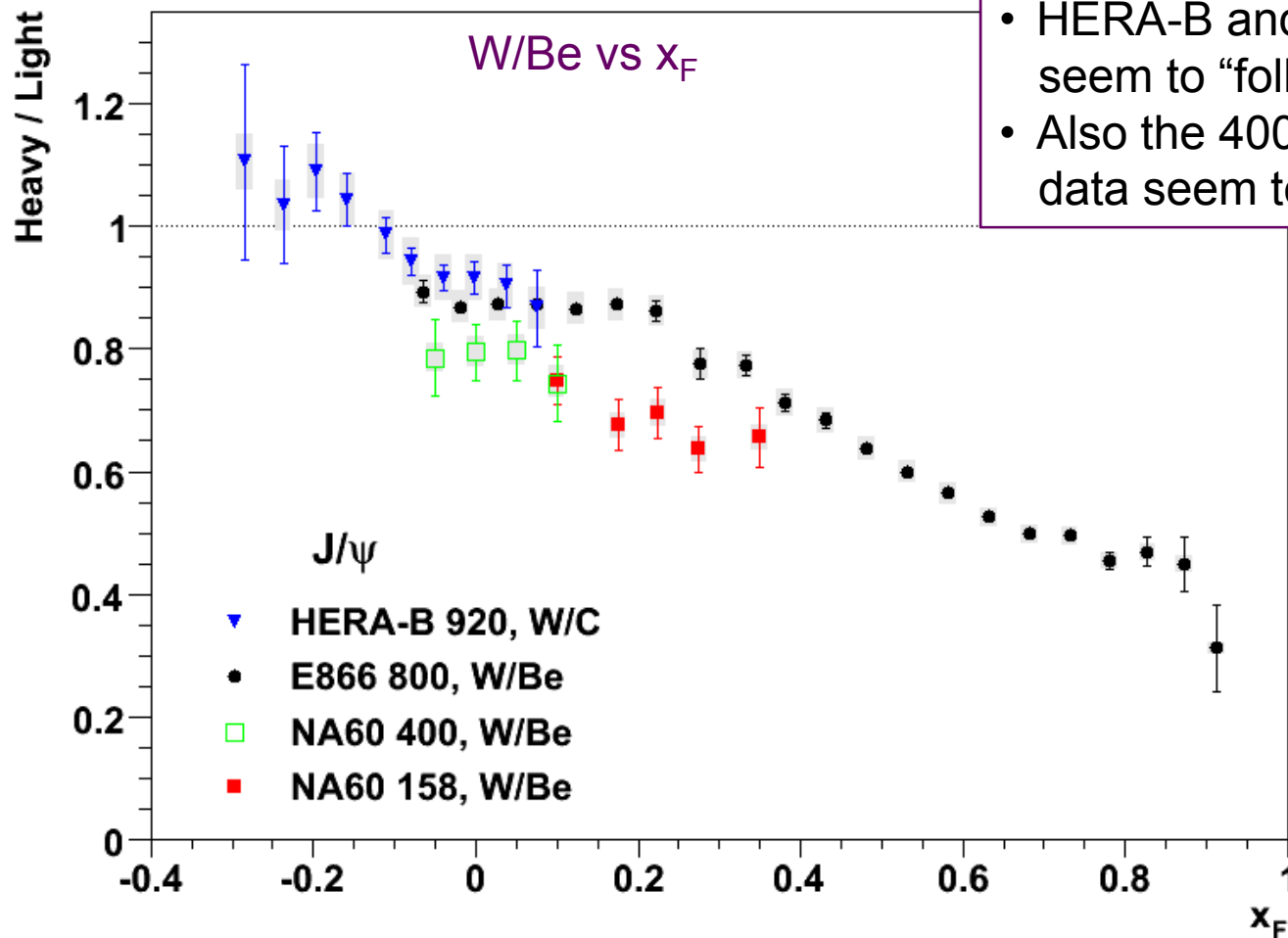


EPS09 uncertainty: NA3 and HERA-B cases



Another look at the measurements

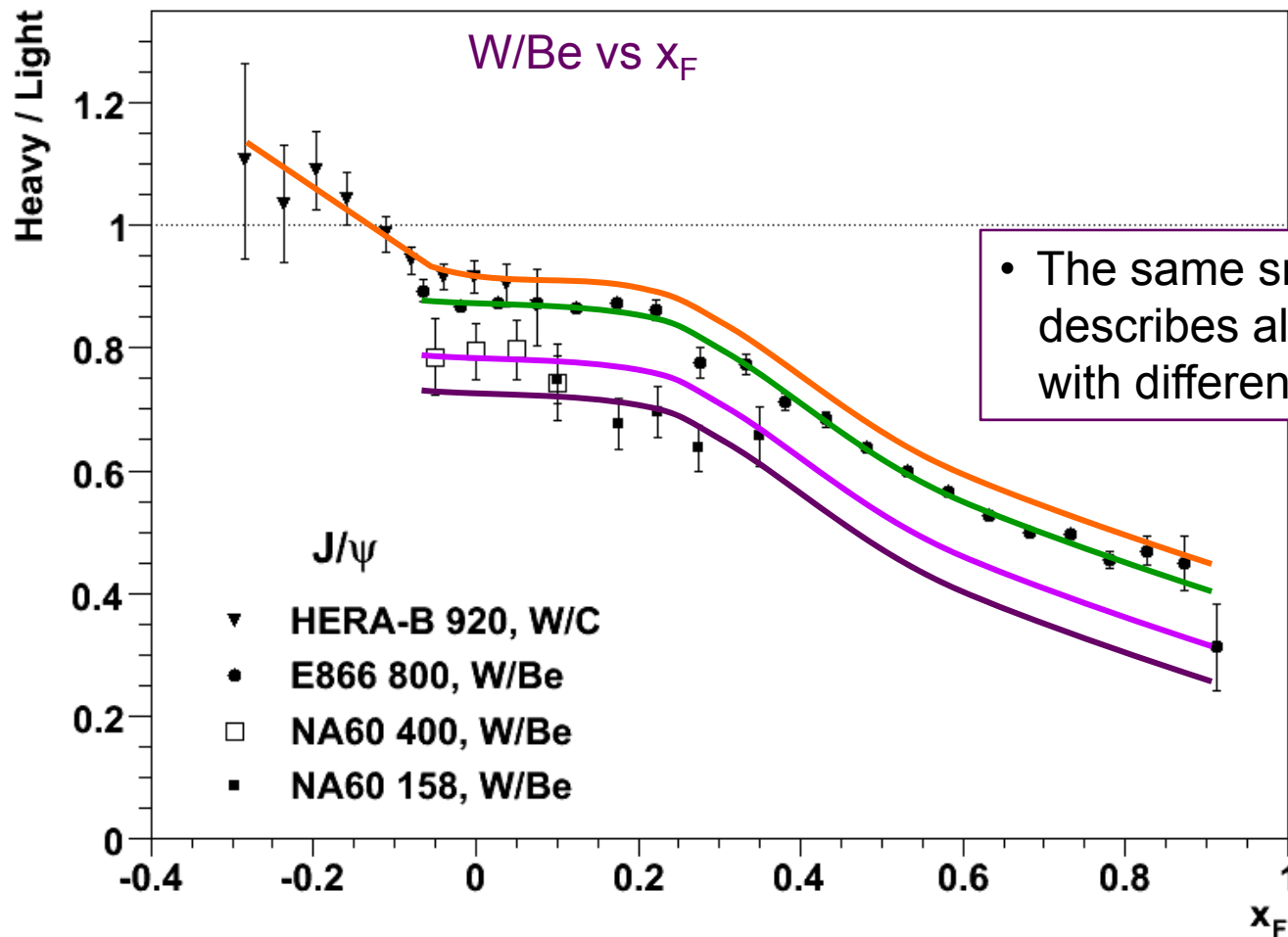
Since there are several different mechanisms affecting J/ψ production in p-nucleus collisions and it is unreasonable to convolute them all in a single “effective variable”, let’s go back to the data, to search for scaling features and inspiration...



- HERA-B and E866 patterns seem to “follow each other”
- Also the 400 and 158 GeV data seem to be well “aligned”

Another look at the measurements

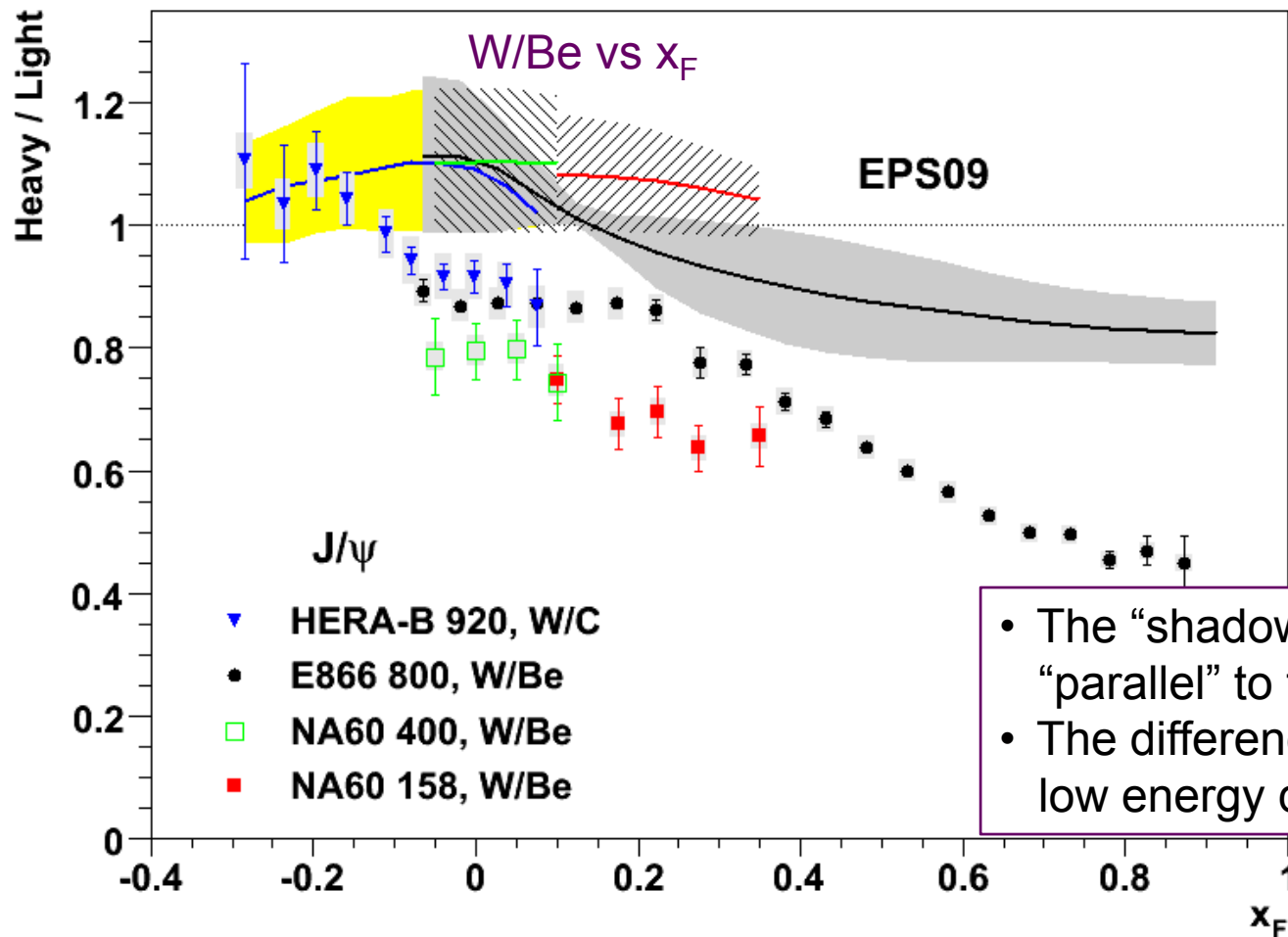
Since there are several different mechanisms affecting J/ψ production in p-nucleus collisions and it is unreasonable to convolute them all in a single “effective variable”, let’s go back to the data, to search for scaling features and inspiration...



- The same smooth pattern describes all the four data sets with different normalisations

Another look at the measurements

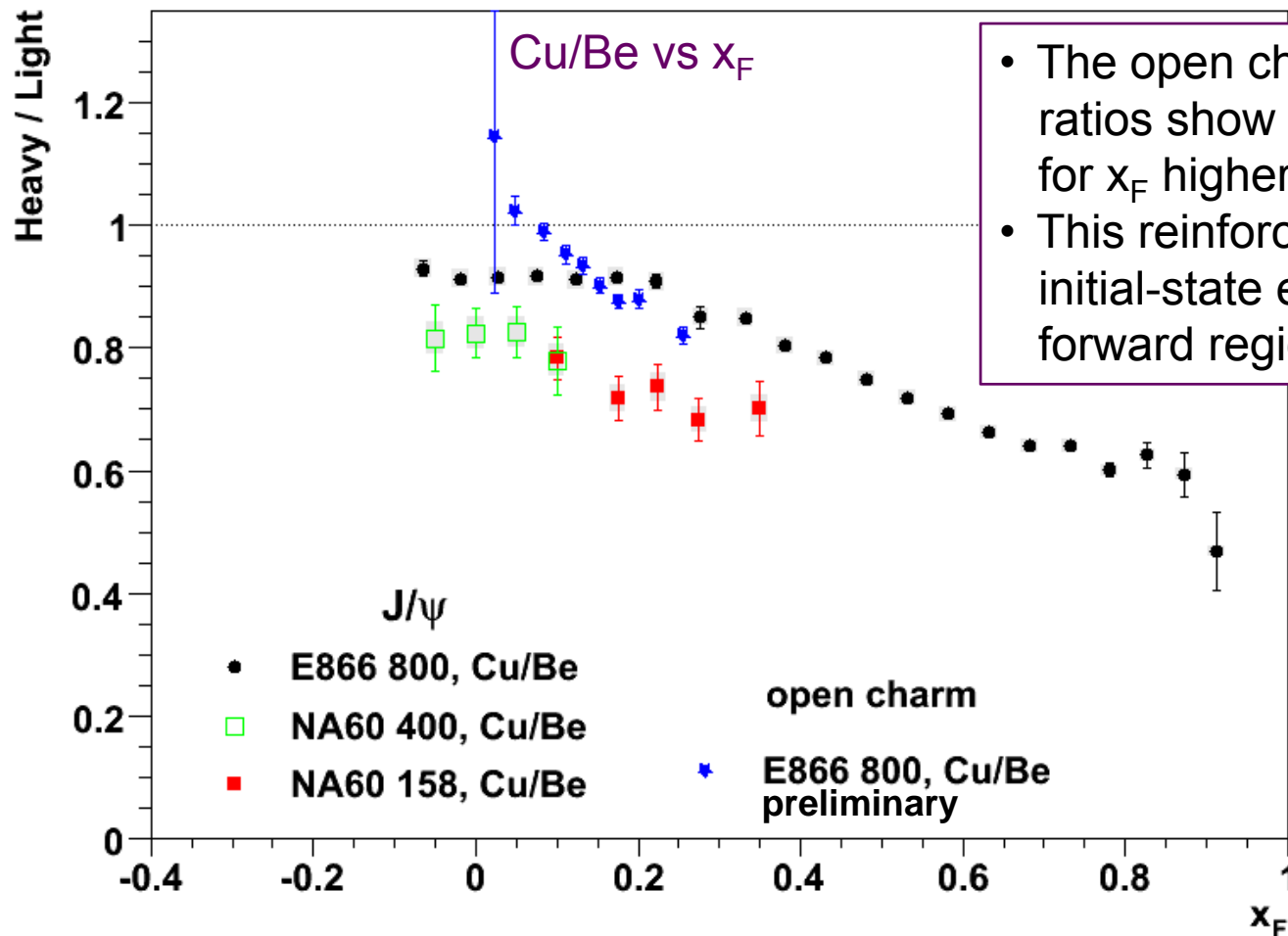
Since there are several different mechanisms affecting J/ψ production in p-nucleus collisions and it is unreasonable to convolute them all in a single “effective variable”, let’s go back to the data, to search for scaling features and inspiration...



- The “shadowing” curves are not “parallel” to the measured patterns
- The difference is larger for the low energy data sets

Another look at the measurements

Since there are several different mechanisms affecting J/ψ production in p-nucleus collisions and it is unreasonable to convolute them all in a single “effective variable”, let’s go back to the data, to search for scaling features and inspiration...



- The open charm and J/ψ Cu / Be ratios show a similar decrease for x_F higher than ~ 0.15
- This reinforces the idea that initial-state energy loss drives the forward region

Summary

- There are several different “cold nuclear matter effects” affecting quarkonium production in proton-nucleus collisions
- Our best chance to disentangle them is to perform a global study of many sets of nuclear dependent measurements, including J/ψ , ψ' and χ_c mesons, but also open charm and Drell-Yan, as a function of kinematics, collision energy, etc
- What can we learn from the p_T dependence, not addressed so far?
- Only once we have a model incorporating initial state parton energy loss, shadowing, formation time effects, final state break-up, ... we will have a proper understanding of J/ψ production in nuclear targets.

This could help disentangling colour singlet vs. colour octet production

Some J/ψ data we have considered

	$B \times \sigma^{J/\psi} / A$ [nb/nucleon]		
	NA50-400	NA50-450 “LI”	NA50-450 “HI”
Be	4.717 ± 0.10	5.27 ± 0.23	5.11 ± 0.18
Al	4.417 ± 0.10	5.14 ± 0.21	4.88 ± 0.23
Cu	4.280 ± 0.09	4.97 ± 0.22	4.74 ± 0.18
Ag	3.994 ± 0.09	4.52 ± 0.20	4.45 ± 0.15
W	3.791 ± 0.08	4.17 ± 0.37	4.05 ± 0.15
Pb	3.715 ± 0.08		

NA3	
x_F range	H / Pt ratio
0.0 / 0.1	1.27 ± 0.07
0.1 / 0.2	1.40 ± 0.06
0.2 / 0.3	1.34 ± 0.07
0.3 / 0.4	1.36 ± 0.12
0.4 / 0.5	1.75 ± 0.22
0.5 / 0.6	2.62 ± 0.52
0.6 / 0.7	3.58 ± 1.81



HERA-B			
x_F range	$\langle x_F \rangle$	W / C ratio	
−0.34 / −0.26	−0.285	1.105 ± 0.158	
−0.26 / −0.22	−0.237	1.034 ± 0.096	
−0.22 / −0.18	−0.197	1.090 ± 0.063	
−0.18 / −0.14	−0.158	1.043 ± 0.042	
−0.14 / −0.10	−0.118	0.986 ± 0.030	
−0.10 / −0.06	−0.079	0.943 ± 0.022	
−0.06 / −0.02	−0.040	0.915 ± 0.021	
−0.02 / +0.02	−0.002	0.916 ± 0.025	
+0.02 / +0.06	+0.037	0.902 ± 0.036	
+0.06 / +0.14	+0.075	0.866 ± 0.063	

E866		
x_F range	$\langle x_F \rangle$	W / Be ratio
−0.10 / −0.05	−0.0652	0.8929 ± 0.0184
−0.05 / 0.00	−0.0188	0.8682 ± 0.0084
0.00 / +0.05	+0.0269	0.8720 ± 0.0060
+0.05 / +0.10	+0.0747	0.8739 ± 0.0057
+0.10 / +0.15	+0.1235	0.8652 ± 0.0067
+0.15 / +0.20	+0.1729	0.8725 ± 0.0100